Review

Fullerene-Perylenediimide (C$_{60}$-PDI) Based Systems: An Overview and Synthesis of a Versatile Platform for Their Anchor Engineering

Aurel Diacon [1,2], Oksana Krupka [1,3] and Piétrick Hudhomme [1,*,†]

1 Univ. Angers, CNRS, MOLTECH-Anjou, SFR MATRIX, F-49000 Angers, France
2 Department of Bioresources and Polymer Science, Faculty of Chemical Engineering and Biotechnologies, University Politehnica of Bucharest, 1-7 Gh. Polizu Street, 011061 Bucharest, Romania
3 Department of Chemistry, Taras Shevchenko National University of Kyiv, 60 Volodymyrska, 01033 Kyiv, Ukraine
* Correspondence: pietrick.hudhomme@univ-angers.fr; Tel.: +33-2-4173-5094
† Dedicated to Professor Alain Gorgues for his 80th birthday.

Abstract: An overview of the different covalent bonding synthetic strategies of two electron acceptors leading to fullerene-perylenediimide (C$_{60}$-PDI)-based systems, essentially dyads and triads, is presented, as well as their more important applications. To go further in the development of such electron and photoactive assemblies, an original aromatic platform 5-benzyloxy-3-formylbenzoic acid was synthesized to graft both the PDI dye and the fullerene C$_{60}$. This new C$_{60}$-PDI dyad exhibits a free anchoring phenolic function that could be used to attach a third electro- and photoactive unit to study cascade electron and/or energy transfer processes or to obtain unprecedented side-chain polymers in which the C$_{60}$-PDI dyads are attached as pendant moieties onto the main polymer chain. This C$_{60}$-PDI dyad was fully characterized, and cyclic voltammetry showed the concomitant reduction process onto both C$_{60}$ and PDI moieties at identical potential. A quasi-quantitative quenching of fluorescence was demonstrated in this C$_{60}$-PDI dyad, and an intramolecular energy transfer was suggested between these two units. After deprotection of the benzyloxy group, the free hydroxyl functional group of the platform was used as an anchor to reach a new side-chain methyl methacrylate-based polymer in which the PDI-C$_{60}$ dyad units are located as pendants of the main polymer chain. Such polymer which associates two complementary acceptors could find interesting applications in optoelectronics and in particular in organic solar cells.

1. Introduction

Photosynthetic and photovoltaic processes harvest energy from sunlight, but they operate in distinctly different ways to produce biomass or chemical fuels in the case of natural photosynthesis and electrical current in the case of photovoltaics [1]. The possibility to generate energy and/or electron transfer and long-lived charge-separated states using fullerenes as electron acceptors has rapidly shown their great advantages to be used in artificial photosynthetic models and organic molecular electronics including solar cells [2]. This story began with the discovery in 1985 by H. Kroto et al. of fullerene C$_{60}$ [3], and this allotropic form of carbon then sparked the imagination of organic chemists who used its nano-sized football geometry as a new Lego® block. The large-scale production in the early 1990s was the first breakthrough [4,5] that allowed the development of chemical methodologies to functionalize C$_{60}$. This has made C$_{60}$ a fascinating molecule for building molecular assemblies with remarkable physical and chemical properties, leading to a wide range of interesting applications, from materials to medicinal sciences [6,7]. In particular, its electrochemical properties with six reversible single-electron reduction waves [8], combined

with interesting photophysical properties, make C_{60} a unique electron acceptor to study photoinduced electron transfer processes.

In particular, the ability of a pi-conjugated polymer to efficiently transfer electrons to C_{60}, giving rise to long-lived charge-separated states [9], has suggested that fullerene derivatives could be used for photovoltaic applications [10]. This was the starting point for the explosion of interest in their use as materials in the active layer of organic solar cells (OSCs). The synthesis by F. Wudl and coll. in 1995 of a functionalized C_{60} derivative, named [6,6]-phenyl-C_{61}-butyric acid methyl ester $PC_{61}BM$) [11], paved the way for the great development of organic photovoltaics (OPVs) using the polymer/fullerene bulk-heterojunction (BHJ) concept [12]. The construction of BHJ devices consists in mixing together donor and acceptor materials to form a bicontinuous interpenetrating network and they have attracted much attention as they offer the possibility to achieve high power conversion efficiencies (PCE). Thanks to their geometrical tridimensional architecture, good electron mobility, excellent electron properties, and good miscibility with conductive polymers, fullerene derivatives were considered for two decades as the spearhead of the acceptors for the development of OPVs [13]. However, despite these promising characteristics, fullerene-based OSCs exhibited serious drawbacks, including poor light-absorption properties, limited energy-level tunability, and significant morphological and/or photochemical instability [14]. To overcome these limitations, tremendous efforts have been directed toward the synthesis of non-fullerene acceptors (NFAs), especially small molecular acceptors (SMAs), and their development in related OSCs [15–19]. Their main advantage is their easily tunable energy levels and better absorption properties giving significantly higher open-circuit voltages (V_{OC}) and photocurrents (J_{SC}), respectively, than conventional fullerene-based devices. Last, SMAs with proper molecular design can also be more chemically stable, thus extending the device lifetime of OSCs [20].

On the front of applications involving fullerenes under the influence of light irradiation, energy and electron transfer processes are essential photochemical events in photosynthesis [21]. The conversion of solar energy into chemical energy is initiated by the light-harvesting of various chromophores, so-called antenna complexes, and the funneling of the produced exciton by energy transfer to a specific site, known as the reaction center, in which a subsequent electron transfer to an electron acceptor can occur [22,23]. The mimicry of natural photosynthesis by artificial systems holds the promise for cheap, environmentally friendly energy generation. Consequently, the incorporation of artificial light-harvesting antennas into molecular electron donor–acceptor systems was regarded as one of the most interesting strategies for the design of optoelectronic materials in photon-energy conversion. In this area, the covalent bonding of a light-harvester, capable to act as an electron donor, to C_{60} has emerged as an active field of research to reach dyads in which intramolecular electronic interactions dominate generating a long-lived charge-separated state [24].

Among these materials capable to act as light-harvesting absorbers, the iconic perylenediimide (PDI) presents many advantages since this photoactive molecule exhibits high chemical, thermal and photochemical stability, wide and intense optical absorption in the visible to near-infrared spectral window, high photoluminescence quantum yield, and excellent charge transport properties [25,26]. These PDI derivatives are of great interest to be studied as alternative electron acceptors to fullerenes in OPVs due to their tunable absorption in the visible range, inexpensive synthesis, and photochemical stability [27–30]. Moreover, the idea of covalently linking the fullerene with PDI quickly became obvious in order to create dyad systems that were rapidly considered as light-harvesting fullerenes in the search for photoinduced electron and/or energy transfer processes. These systems present high potential to be used in OSCs [31] or as organic triplet photosensitizers with potential applications in photocatalysis, photooxidation, and photodynamic therapy or for artificially mimicking the photosynthesis phenomenon [32].

This presentation aims to highlight the different synthetic strategies elaborated to build C_{60}-PDI-based systems and their potential for applications in materials chemistry (Section 2). Moreover, for the development of such electron and photoactive assemblies, an

original aromatic platform of 5-benzyloxy-3-formylbenzoic acid has been synthesized to graft both the PDI dye and the fullerene C_{60} (Section 3). This new C_{60}-PDI dyad exhibits a free anchoring phenolic function that could be used to attach a third electro- and photoactive unit to study cascade electron and/or energy transfer processes or to obtain unprecedented side-chain polymers in which the C_{60}-PDI dyads are attached as pendant moieties onto the main polymer chain.

2. State-of-the-Art of Covalently Linked C_{60}-PDI Based Systems

This overview focuses on the different synthetic methodologies that have been used so far to graft the PDI unit onto C_{60}. The perylene scaffold has three different types of functionalizable positions. The 3,4,9, and 10 positions known as the *peri* positions correspond to the diimide functions for PDI derivatives (Figure 1) [33]. The introduction of substituents at this imide nitrogen atoms significantly improves the solubility of the corresponding materials. The other positions 1,6,7, and 12, called *bay* positions, and 2,5,8, and 11 *ortho* positions play a key role in tuning their optical and electronic properties. Considering the recent development of functionalization on *ortho* positions, to our knowledge no C_{60}-PDI dyad has been reported to date considering this possibility. Therefore, we will only consider the development of strategies to attach C_{60} to the imide position or the bay region of the PDI core.
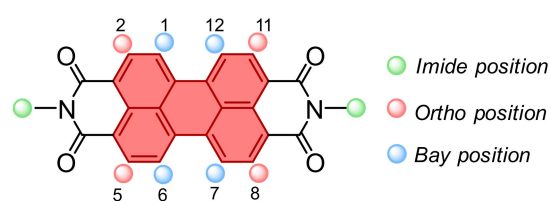
Figure 1. Strategies for functionalization of perylenediimide (PDI) scaffold.

Among the different strategies available for the functionalization of C_{60} fullerene, it should be noted beforehand that most of the examples described here involve the [2 + 1] and [3 + 2] cycloadditions, more commonly known as the Bingel [34] and Prato [35] reactions, respectively.

To carry out the Prato reaction, an amino acid derivative, most often N-methylglycine (sarcosine), reacts with an aldehyde in refluxing toluene (chlorobenzene or *o*-dichlorobenzene can also be used) to generate an azomethine ylide which interacts with a 6:6-double bond in a 1,3-dipolar cycloaddition to yield the N-methylpyrrolidine derivative.

The Bingel reaction can be carried out on α-halomalonate in the presence of a base to firstly generate the corresponding anion which adds to C_{60} via an addition–elimination process by intramolecular displacement of the halide to give the corresponding methanofullerene. This nucleophilic cyclopropanation is improved by directly using the malonate from which the α-halomalonate is produced in situ in the presence of iodine or CBr_4 and 1,8-diazabicyclo [5.4.0]undec-7-ene (DBU) acting as a base. The reaction using iodine was initially developed by J.-F. Nierengarten and F. Diederich [36], whereas the reaction with CBr_4 is known as the Bingel–Hirsch reaction [37].

2.1. Grafting C_{60} at the Imide PDI Scaffold

Over the past two decades, electro- and photoactive C_{60}-PDI dyads have been synthesized by attaching C_{60} to the imide position. Unlike triad access, which can utilize both symmetrically substituted positions of the PDI motif, the key step for dyad syntheses requires desymmetrization of the PDI scaffold. Starting with 1,6,7,12-tetrakis(4-*tert*-butylphenoxy)perylene dianhydride, the reaction of ammonia and *n*-butylamine afforded the asymmetric PDI derivative. After alkylation to introduce the aldehyde linker, the Prato reaction with C_{60} and sarcosine was used by H. Tian and coll. to obtain dyad **Aa** (Scheme 1) [38]. Electrochemical and photophysical studies in solution revealed that there is no significant ground-state electronic interaction between both PDI and C_{60} partners. These

studies have shown that singlet-singlet energy transfer from the PDI unit to C_{60} occurs predominantly in dyad **Aa**. A photovoltaic device using this dyad confirmed that the efficiency of the photoinduced electron transfer is negligible compared to energy transfer. Using this methodology, symmetrical C_{60}-PDI-C_{60} dumbbell **Ab** was prepared and found to exhibit good solubility, high thermal stability, and broad visible-light absorption [39]. Photophysical studies confirmed the presence of a photoinduced energy transfer from the PDI moiety to C_{60}.
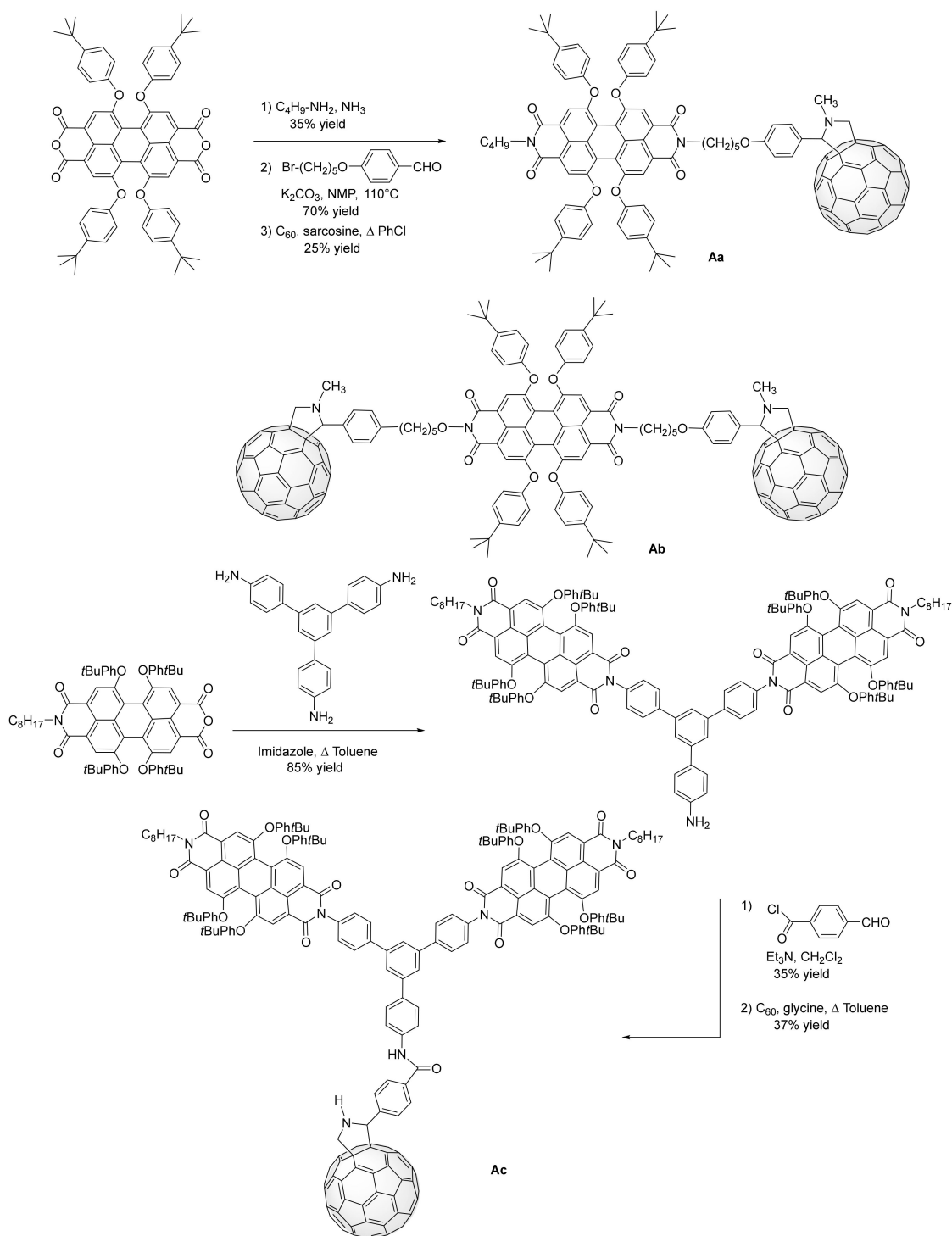
Scheme 1. Synthesis of PDI-C_{60} dyad **Aa** and C_{60}-PDI-C_{60} dumbbell **Ab** by H. Tian and coll., triad PDI-C_{60}-PDI **Ac** by D. Zhu and coll.

Using this highly soluble perylene dianhydride, D. Zhu and coll. developed a synthetic route to reach PDI-C$_{60}$-PDI triad **Ac** [40]. Firstly, the unsymmetrically substituted PDI is classically synthesized from the corresponding *N,N'*-dialkyl-1,6,7,12-tetrakis(4-*tert*-butylphenoxy)PDI which is hydrolyzed in basic medium leading to a mixture of the perylene monoanhydride and the perylene bisanhydride that are separated by column chromatography [41]. The imidization of the perylene monoanhydride using 1,3,5-tris(4-aminophenyl)benzene [42] was followed by the reaction of the remaining amino functionality with 4-formylbenzoyl chloride. Finally, 1,3-dipolar cycloaddition to C$_{60}$ in the presence of glycine afforded triad **Ac** for which the strong quenching of the PDI fluorescence was suggested to result from an intramolecular photoinduced charge-transfer process within the triad.

Our group, in collaboration with R. M. Williams, was interested in the concept of super-absorbing fullerenes obtained by linking a dye molecule to fullerene C$_{60}$ as new systems exhibiting efficient light-harvesting properties. The objective was to consider that the dye could act as an antenna by absorption of sunlight inducing an intramolecular energy transfer towards the fullerene, playing the role of energy receptor. The corresponding solar cells should be designed considering that inside the photoactive layer the following combination of events could occur: (i) self-assembly into an interpenetrating nanoscopic network, (ii) an energy transfer from PDI towards fullerene C$_{60}$ with the dye acting as a light-harvesting antenna, and (iii) a selective electron transfer between the p-type polymer donor such as poly(3-hexylthiophene) (P3HT) to the C$_{60}$ unit. One of the objectives was to demonstrate that the nature of the substituents on the PDI bay region strongly influences the electronic properties of these dyads for their subsequent use in photovoltaic devices. Furthermore, an interesting feature in the design of these C$_{60}$-PDI dyads was to demonstrate that the distance between PDI and C$_{60}$ moieties and their mutual orientation could be crucial parameters for the energy transfer rate and could play an important role in the electronic interaction between the two partners. The key step in the preparation of dissymmetrical PDI was achieved by direct condensation of 1,6,7,12-tetrachloroperylene dianhydride with two aliphatic amine derivatives of similar reactivity such as pentan-1-amine and 2-aminoethanol or 5-aminopentan-1-ol in stoichiometric ratio and in refluxing toluene [43,44]. After separation from the two symmetric compounds, the subsequent introduction of *tert*-butylphenoxy groups could be carried out on the asymmetric alcohol using an aromatic nucleophilic substitution of chlorine atoms with 4-*tert*-butylphenol in the presence of K$_2$CO$_3$. Transformation of the alcohol to the malonate functionality was performed using ethyl malonyl chloride in the presence of pyridine. The cyclopropanation was carried out by reaction with C$_{60}$ in the presence of iodine and DBU to give corresponding C$_{60}$-PDI dyads **Ba–d** in satisfactory yields (Scheme 2) [45,46].
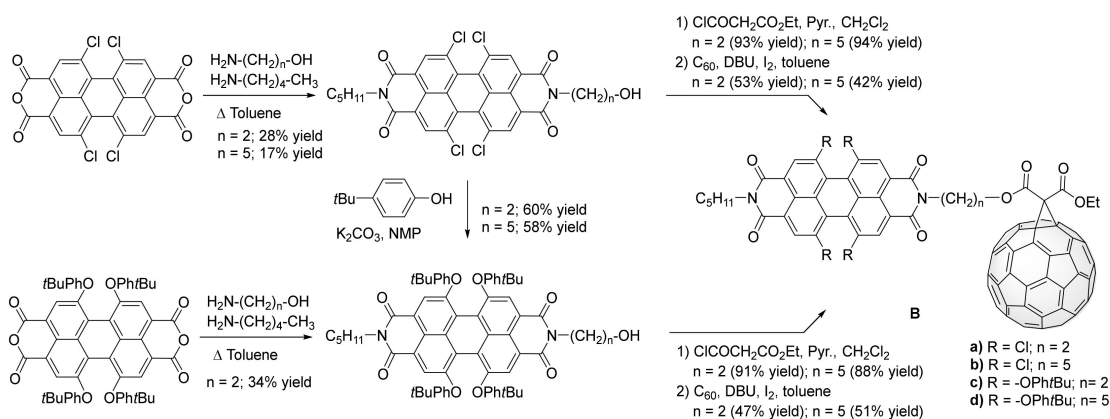

Scheme 2. Synthesis of PDI-C$_{60}$ dyads **Ba–d** developed by P. Hudhomme and coll.

Electronic properties being tuned by an appropriate substitution of the PDI bay region, the first reduction unambiguously occurs on the PDI moiety in the case of dyads **Ba** and **Bb**, but the reduction potentials of the PDI moiety are shifted to more negative values when chlorine atoms were substituted by *tert*-butylphenoxy groups. Consequently, the C_{60} moiety appears to be the favored electron acceptor inside dyads **Bc** and **Bd**. The electron-withdrawing inductive effect of the chlorine atoms stabilizes the anion radical PDI$^{-\cdot}$, whereas the electron-donating mesomeric effect of phenoxy groups appears predominant [47]. The photophysics of C_{60}-PDI systems is also governed by their bay substituents and the distance between the chromophores that mainly determine the presence of energy or electron transfer. It was shown in solvents of different polarity that C_{60}-PDI systems containing chlorine atoms (**Ba,b**) or *tert*-butylphenoxy groups (**Bc,d**) as bay substituents display an efficient singlet-singlet energy transfer from the PDI unit to C_{60}, thus acting as light-harvesting antenna to the C_{60} playing the role of energy acceptor [46,48,49]. The excited fullerene unit thus created ($^1C_{60}$) displays its characteristic spin-orbit coupling and converts to the triplet state with efficiency close to unity. This $^3C_{60}$ can then act as an intramolecular triplet sensitizer populating the triplet state of the PDI unit. Such PDI compounds that have very high triplet quantum yields and present intramolecular triplet sensitization could yield systems that are very suited for singlet oxygen production for photodynamic therapy applications, especially since the compounds absorb strongly in the 500–700 nm region. The potential use of these light-harvesting fullerenes in OSCs was estimated with their incorporation in BHJ using P3HT as the pi-conjugated donor polymer. The role of a light-harvesting antenna grafted onto C_{60} was demonstrated thanks to the presence of an efficient energy transfer from the PDI towards fullerene C_{60}. Moreover, the photovoltaic behavior was in agreement with electrochemical data which showed that PDI should be favored to play the role of acceptor instead of C_{60} in dyad **Bc** with a higher efficiency compared to the device using dyad **Ba** [50].

This strategy for bay-PDI desymmetrization, using the statistical imidization reaction with two different amines on the perylene dianhydride [43,44,51], was applied by A. Sastre Santos and coll. to prepare dyad **C** [52]. Introduction of the formyl derivative using a copper-catalyzed azide-alkyne cycloaddition was followed by the Prato 1,3-dipolar cycloaddition to afford linear dyads **Ca** and **Cb** (Scheme 3). Starting from the double condensation of 3-azido-1-propylamine, the PDI diazide derivative was used as a precursor of macrocyclic dyad **Da** and **Db** obtained as a mixture of regioisomeric C_{60} cycloadducts. It was noted that compound **Da** was accompanied with the symmetrical linear C_{60}-PDI-C_{60} triad. Photophysical studies showed a photoinduced energy transfer from ^{1}PDI* to C_{60} which was followed by intersystem crossing from $^1C_{60}$* to $^3C_{60}$* in the case of PDICl$_4$-C_{60} dyads that is, in particular, one order of magnitude faster in the cyclic dyad **D** compared to the linear one **C**. Using these intermediates and synthetic strategies, the electron donor silicon phthalocyanine (SiPc) was incorporated between the two electron acceptors of the multichromophoric PDI-SiPc-C_{60} triad **Ea** [53]. An ultrafast singlet-singlet energy transfer from ^{1}PDI* to SiPc ultimately led to the two PDI-SiPc$^+$-C_{60}^- and PDI.$^-$SiPc$^+$-C_{60} charge-separated states. Compared to the triad **Eb**, it was shown that the spacer length plays an important role in governing the excited state energy and the electron transfer events [54].

To prevent through-space interaction and with the aim of possibly enhancing the energy transfer process, both C_{60} and PDI partners were linked by a rigid biphenyl spacer allowing a fixed spatial distance between them. The synthesis of dyad **Fa** carried out by X.-F. Wang, G.-W Wang and coll. involves a 1,3-dipolar cycloaddition of the azomethine ylide generated in situ from the condensation of the glycinate group with C_{60} (Scheme 4) [55]. Triad **Fb** was prepared by imidization of the perylene dianhydride in 44% yield. In fact, an efficient intramolecular energy transfer from PDI antenna to C_{60} is followed by an intrinsic intersystem crossing of C_{60} leading to the production of C_{60} triplet. This property of a light-harvesting antenna combined with an intersystem crossing was used as an efficient photooxidation system for the transformation of 1,5-dihydroxynaphthalene into juglone,

showing that the C_{60}-PDI dyad could be used as a triplet photosensitizer. The presence of two C_{60} units showed a 1.3-fold increase in the efficiency of **Fb** compared to that of **Fa**.
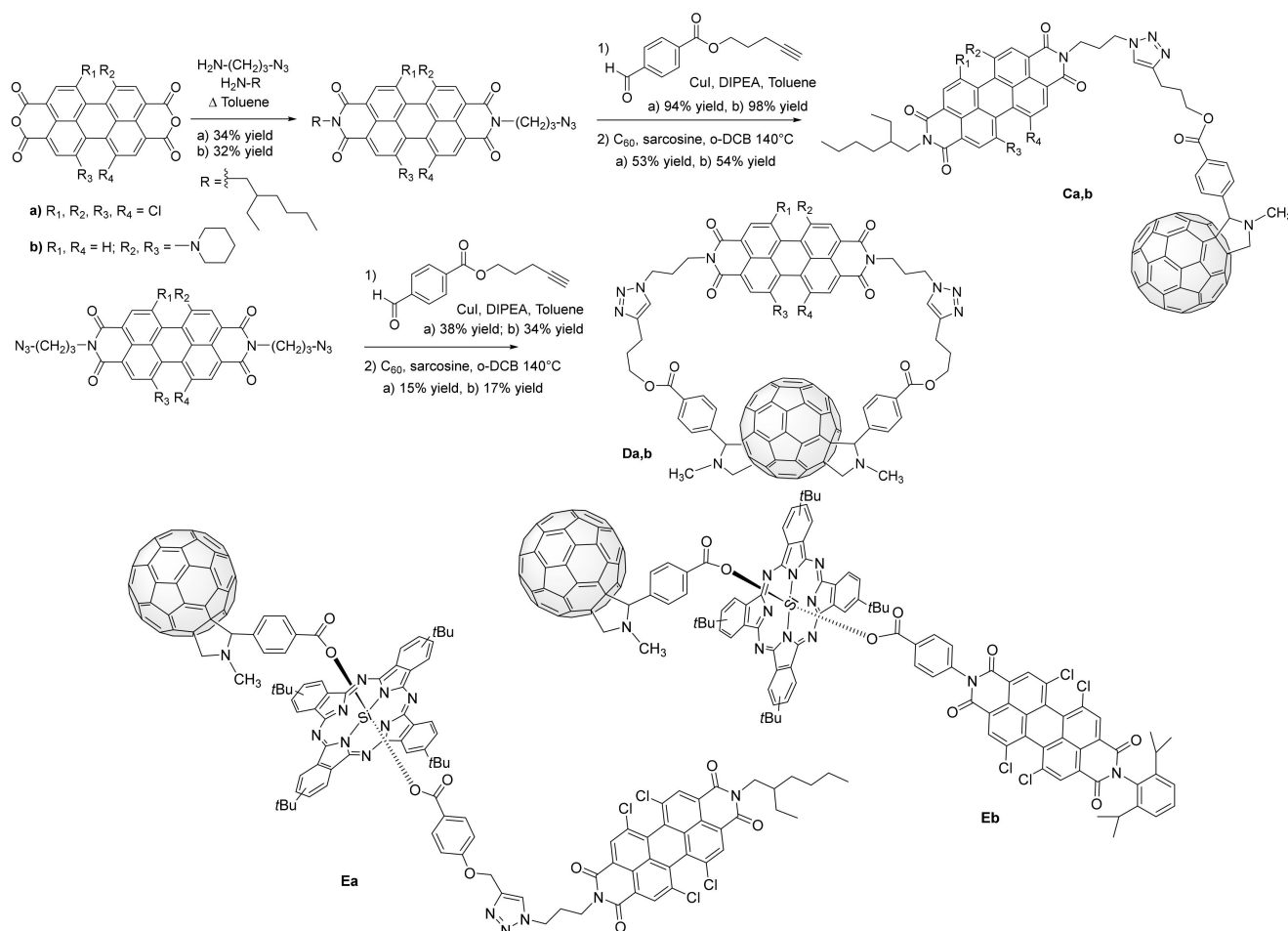
Scheme 3. Synthesis of linear PDI-C_{60} dyads **C**, macrocyclic PDI-C_{60} dyad **D** and extension to multichromophoric PDI-SiPc-C_{60} triads **Ea** and **Eb** by A. Sastre Santos and coll.

　　　Very recently, A. Hirsch and coll. described the synthesis of dumbbell-like molecules and PDI-cyclophanes functionalized with fullerenes (Scheme 5) [56,57]. Starting from the PDI dialcohol, the bis-malonate was prepared using dimalonyl chloride in the presence of pyridine as a base. Whereas the experimental conditions were using the couple iodine and DBU for cyclopropanation of C_{60} with the corresponding malonate, the typical Bingel-Hirsch conditions (CBr$_4$/DBU) were used when using C_{60} pentakisadducts [58]. Nevertheless, in the latter case, to overcome the low yield to afford dumbbell **G**, DBU was efficiently replaced by the Schwesinger phosphazene base (P$_1$-*t*Bu) for the in situ generation of the α-bromomalonate intermediate [59]. On the other hand, the preparation of the cyclophane was carried out from the PDI dialcohol with malonyl dichloride. The Ziegler–Ruggli principle, taking place under high dilution conditions, was applied to avoid polymerization reactions and to promote intramolecular ring closure. Additionally, the electron-donor tetrathiafulvalene (TTF) was added to the mixture to favor a template-controlled synthesis thanks to the promotion of a pre-arranged sandwich-like structure. To carry out in a satisfactory way the cyclopropanation affording assemblies **H**, the P$_1$-*t*Bu base was associated either with iodine in toluene for **Ha** using pristine C_{60} or CBr$_4$ in CH_2Cl_2 in the case of C_{60} pentakisadducts **Hb** bearing ethyl or tetraethylene glycol (TEG) groups.
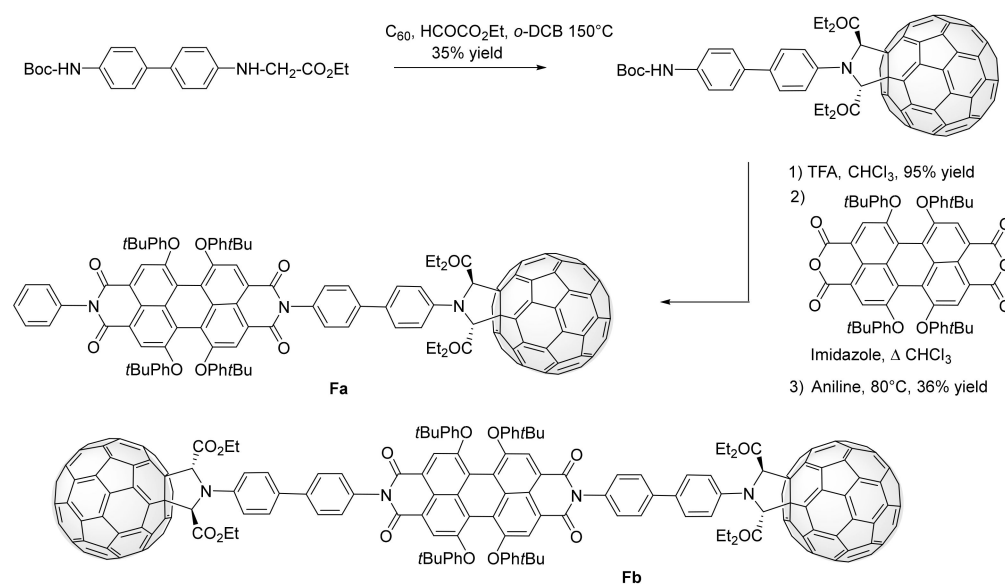
Scheme 4. Introduction of a rigid spacer in C_{60}-PDI dyad **Fa** and PDI-C_{60}-PDI triad **Fb** by G.-W. Wang and coll.

Bay-substituted PDI are twisted due to the steric hindrance of their substituents with the possible existence of two (*M/P*) atropoisomers (Scheme 5) [60]. In the case of 4-*tert*-butylphenoxy groups in the 1,6,7,and 12 positions, the $M \leftrightarrow P$ interconversion is known to be fast at room temperature [61]. Whereas fast atropoisomerization was observed in ^{1}H-NMR spectra for the linear PDI-bismalonate, this was shown to be slow at the NMR timescale for the PDI-cyclophane. The resulting diastereoisomers *MM/PP* and *MP/PM* were found in a 10:1 ratio, respectively, in $C_2D_2Cl_4$ at $-15\ °C$ as a result of attractive $\pi-\pi$ interactions between the two PDI moieties [56]. It was noted that the co-facial $\pi-\pi$ stacking arising in the PDI-cyclophane-$(C_{60})_2$ **Hb** bearing ethyl groups leads to a complete diastereoselectivity. Moreover, the physico-chemical properties are also governed by these $\pi-\pi$-interactions between PDI units in the cyclophane and the bulky tetrakis(4-*tert*-butylphenoxy) substituents suppress the tendency towards aggregation [62]. On the other hand, starting from dumbbell-like molecule **Ga** and PDI-cyclophane-$(C_{60})_2$ **Ha**, pseudorotaxanes with [10]cycloparaphenylene ([10]CPP) were investigated using NMR and fluorescence spectroscopies, but also the calorimetric (ITC) method, to determine the binding stoichiometries as well as the thermodynamic and kinetic parameters. It was observed that the formation of 1:1 or 1:2 complexes in *o*-DCB depends on the stoichiometry of added [10]CPP, thus demonstrating that the rigidity of **Ha** has no influence on the supramolecular interaction with [10]CPP [57].

The introduction of pyrrolidinyl groups on the bay positions allows the PDI core to act as a donor and consequently undergo an electron transfer towards C_{60}. In this way, electron-rich PDI-C_{60} dyad **I** was synthesized by N. V. Tkachenko, H. Imahori and coll. using the desymmetrization strategy applied on 1,7-dipyrrolidinyl perylene dianhydride. After a three-step synthesis leading to a PDI aldehyde, the following 1,3-dipolar cycloaddition afforded PDI-C_{60} dyad **I** (Scheme 6) [63]. Photo-induced electron transfer was shown to occur from the PDI excited singlet state to C_{60}, generating the corresponding charge-separated state in polar solvents (benzonitrile, pyridine, and *o*-DCB). In contrast, singlet-singlet energy transfer takes place from the PDI to C_{60} in nonpolar solvent (toluene), followed by an intersystem crossing to the C_{60} excited triplet state and a subsequent triplet-triplet energy transfer to yield the PDI excited triplet state [64]. N. V. Tkachenko, A. Sastre Santos and coll. prepared 1,7-dipyrrolidinyl PDI-C_{60} double-bridged dyad **J** using a modified Bingel cyclopropanation [65]. This dyad undergoes an electron transfer in polar

(benzonitrile) and nonpolar (toluene) solvents showing that these dyads behave as artificial photosynthetic models in terms of charge separation.
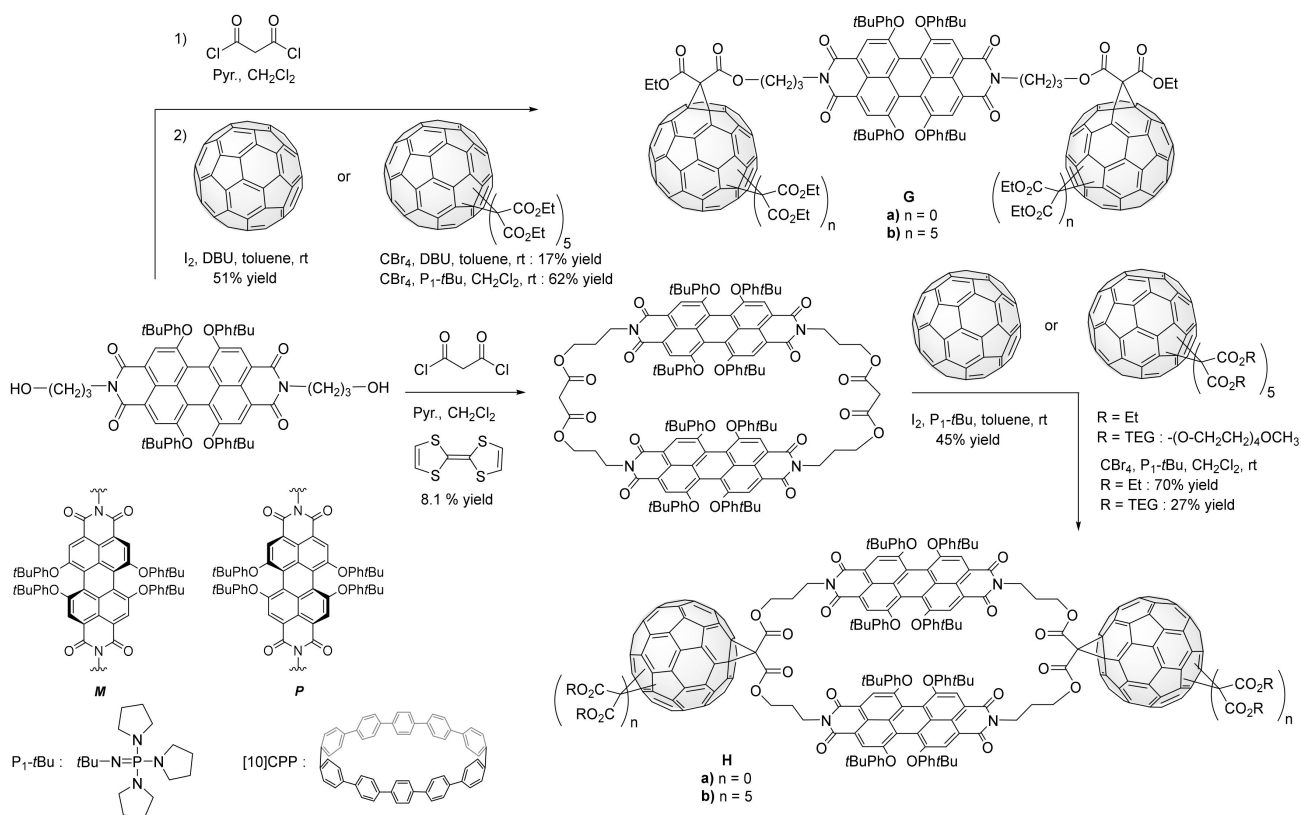

Scheme 5. Dumbbell-like molecules **G** and PDI-cyclophanes functionalized with C$_{60}$ **H** by A. Hirsch and coll.
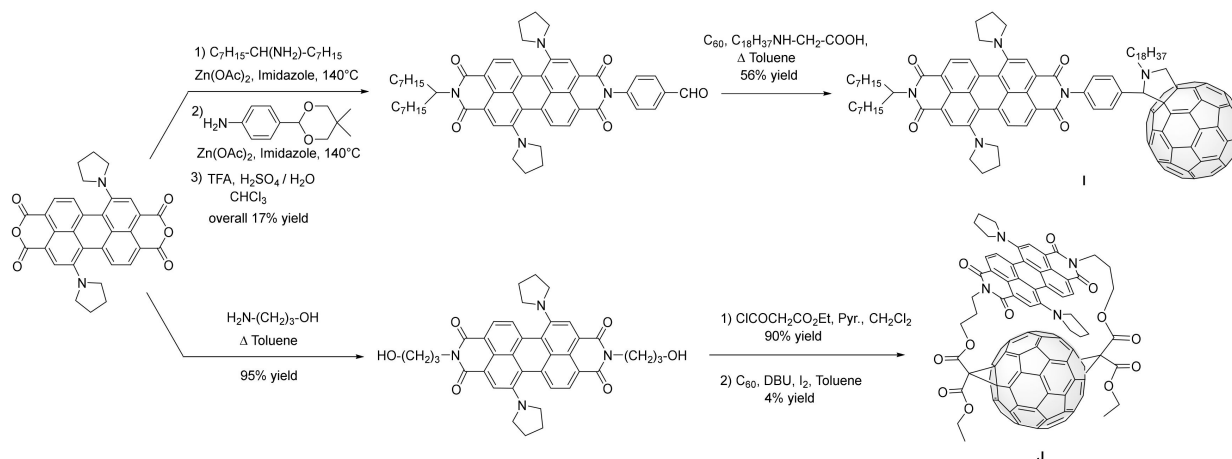
Scheme 6. Linear and double-bridged 1,7-pyrrolidinylPDI-C$_{60}$ dyads **I** and **J**, respectively, prepared by N. V. Tkachenko with H. Imahori, A. Sastre Santos and coll.

　　　For PDI unsubstituted on the bay region, the alternative for desymmetrization consists in the preparation from perylene dianhydride (PTCDA) of the PDI monoanhydride derivative [66]. This strategy was used by J. Köhler and coll. to prepare C$_{60}$-PDI dyad **K** for which a near 100% energy transfer occurs from PDI to C$_{60}$. The fullerene in turn undergoes an intersystem crossing followed by a triplet energy back transfer to the antenna

with an efficiency of at least 20% [67]. The initial synthesis of the key dissymmetrical PDI intermediate was obtained by imidization on the anhydride function, followed by alkylation with protected 6-bromohexanol. The deprotected alcohol function was esterified and the resulting malonate was submitted to a final modified Bingel cycloaddition to give dyad **K** (Scheme 7).
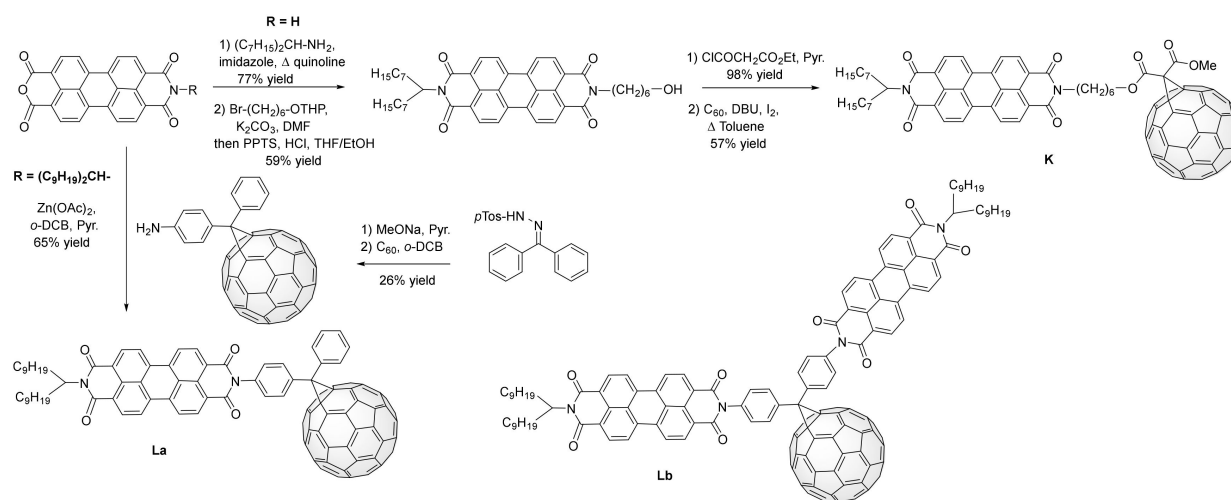
Scheme 7. Synthetic strategies for unsubstituted PDI-C$_{60}$ dyad **K** by J. Köhler and coll, dyad **La** and triad **Lb** by J.L. Segura, N. Martín and coll.

On the contrary, J. L. Segura, N. Martín and coll. have used the Bamford–Stevens reaction to prepare diphenylmethanofullerene-PDI dyad **La** and corresponding triad **Lb** [68]. This cycloaddition reaction is known to transform tosylhydrazones into alkenes under strong basic conditions [69]. It was firstly applied in fullerene chemistry for the synthesis of famous PC$_{61}$BM [11] and [PC$_{71}$BM [70] fullerene derivatives. The critical step corresponds to the transformation of a *p*-toluenesulfonylhydrazide into a diazoalcane intermediate in basic medium using sodium methoxide in pyridine. In a one-pot procedure, trapping with C$_{60}$ in refluxing *o*-DCB via a 1,3-dipolar cycloaddition afforded the open 5:6-fulleroid, as the kinetic product, which was not isolated. The latter was converted in situ into the 6:6-closed methanofullerene as the more stable compound. The perfect match between the excitation and the absorption spectrum strongly suggests a quantitative energy transfer for dyad **La** and triad **Lb** for which a quenching of fluorescence, 99% and 95%, respectively, was observed.

### 2.2. Grafting C$_{60}$ onto Bay-PDI Backbone

The introduction of C$_{60}$ on the bay PDI region was initiated by D. Zhu and coll. with preparation of dyads **Ma** and **Mb** by nucleophilic substitution using a fulleropyrrolidine bearing a phenol group onto 1-bromoPDI or 1,7-dibromoPDI in the presence of K$_2$CO$_3$ and 18-crown-6 (Scheme 8) [71,72]. After this first moderately selective substitution, the free bromine atom from **Mb** was substituted to introduce a ferrocene or zinc porphyrin unit giving corresponding triads **Mc** and **Md** with which photovoltaic devices were fabricated. It should be noted that in the Fc-PDI-C$_{60}$ triad, a N-type cascade electron transfer from the ferrocene (Fc) to the PDI and then from the PDI unit to C$_{60}$ was proposed [73]. As an extension of this work, self-assembled monolayers (SAMs) of porphyrin-PDI-C$_{60}$ triad **Me** were constructed on the indium tin oxide (ITO) surface as photoelectrochemical systems. The incorporation of the PDI as an accessory pigment was intended to complement the absorption of the porphyrin taking advantage that light absorption of PDI and porphyrin occurs in complementary regions, giving extended absorption in the visible spectral window [74].

The dibromination of PTCDA classically yields a mixture of 1,6/1,7-dibromo analog in a 1/3 ratio [75]. From this starting material, conjugated polyacetylenes **Mf** bearing PDI

units and pendant C_{60} acceptors were synthesized by D. Zhu and coll [76]. The nucleophilic substitution of the two bromine atoms using 4-iodophenol was subsequently followed by pallado-catalyzed coupling with trimethylsilylethyne in trimethylamine, then desilylation of protecting groups. The acetylene-containing monomers were copolymerized in the presence of 2-(4-ethynyloxyphenyl)-3,4-fulleropyrrolidine [77] with transition metal catalyst $[Rh(nbd)Cl]_2$, this rhodium catalyst being reported to be effective for the polymerization of monosubstituted acetylenes affording high molecular weight stereoregular polymers with the cis C=C backbone. Interestingly, the photocurrent measurement showed that the films of this polyacetylene could produce steady and rapid cathodic photocurrent responses, indicating that efficient charge transfer took place in this polymer.

Starting from a mixture of 1,6/1,7 regioisomers of a dibromoPDI derivative, R.K. Dubey, H. Lemmetyinen and coll. conducted an original study of single and double-bridged pyrrolidino-substituted PDI-C_{60} dyads (Scheme 9) [78]. The first aromatic nucleophilic substitution using 2-(benzyloxymethyl)pyrrolidine (constructed from *L*-Proline) in toluene at 100 °C was found to be an efficient method for bay-PDI desymmetrization. A second reaction with pyrrolidine at 60 °C was followed by deprotection of the hydroxyl group by using BBr_3. The 1,6- and 1,7-regioisomers could then be successfully separated by column chromatography. Each regioisomer was submitted to esterification with ethyl malonyl chloride and finally, C_{60} was linked using the modified Bingel reaction leading to single-bridged dyads **N-1,6** and **N-1,7** for this last crucial step. A similar synthetic methodology was applied to access double-bridged dyads **O-1,6** and **O-1,7** starting from a PDI backbone substituted by two (hydroxymethyl)pyrrolidine groups in relative bay positions. In contrast to the conventional C_{60} attachment at the imide position of dipyrrolidinyl-substituted PDIs presented for dyads **I** and **J** [63], it was clearly demonstrated that these mono- and bis-bay-functionalized PDIs have the advantage of keeping the two interacting moieties significantly much closer together. Due to the electron-donating character of pyrrolidinyl groups, single and double-bridged dyads **N** and **O** exhibited photoinduced electron transfer in a polar medium, and for single-bridged dyads even in a nonpolar medium. A detailed comparative study showed interesting differences in the physical properties of the 1,6- and 1,7-regioisomers for which different orientations of the donor-acceptor moieties were highlighted. Specifically, the single-bridged dyad **N-1,7** displayed highly efficient photoinduced electron transfer in a nonpolar medium, making it attractive for applications in solid OPV and optoelectronics. A P3HT:dyad **N-1,7**-based blend revealed a charge transfer process in thin film taking place firstly from P3HT to the PDI moiety to attain in a second time a charge-separated state $P3HT^+/PDI-C_{60}^-$ before a recombination via hole transfer to the PDI moiety and finally a charge recombination to the ground state [79].

One of the main advantages of the modified Bingel reaction [36,37] which uses malonate as starting material concerns the installation of ester moieties that allows additional chemical transformations. Thus, the key step in the synthesis of asymmetric malonate compounds is the use of Meldrum's acid ring-opening with an alcohol to reach a monoesterified malonic acid derivative. This synthetic methodology was applied by J.-F. Nierengarten, N. Armaroli and coll. to synthesize three generations of fullerodendrimers with a PDI core P_{1-3} (Scheme 10) [80]. Starting from the PDI dialcohol building block obtained by the nucleophilic substitution from 1,7-dibromoPDI [81], the esterification with fullerodendrons [82,83] bearing a carboxylic acid function led to the fullerodendrimers. Electrochemical studies showed that the oxidation of the dendrimers is always centered on the PDI core, while the first reduction always corresponds to fullerene units. Moreover, photophysical properties evidenced that a photosensitization process occurs within the dendrimers P_{1-3} via photoinduced energy transfer leading to long-lived triplet states centered on a dendrimer core and capable of sensitizing singlet oxygen.
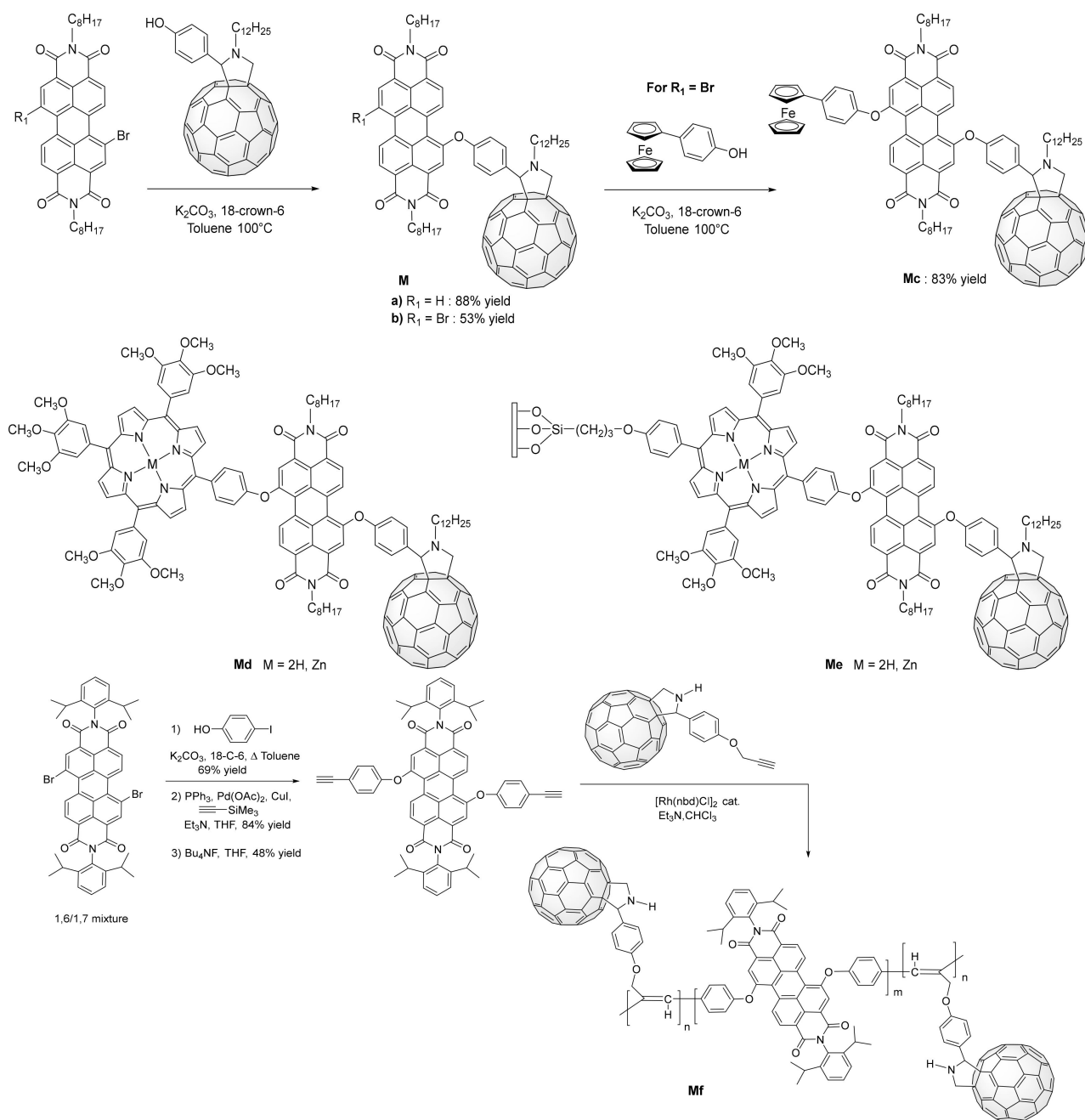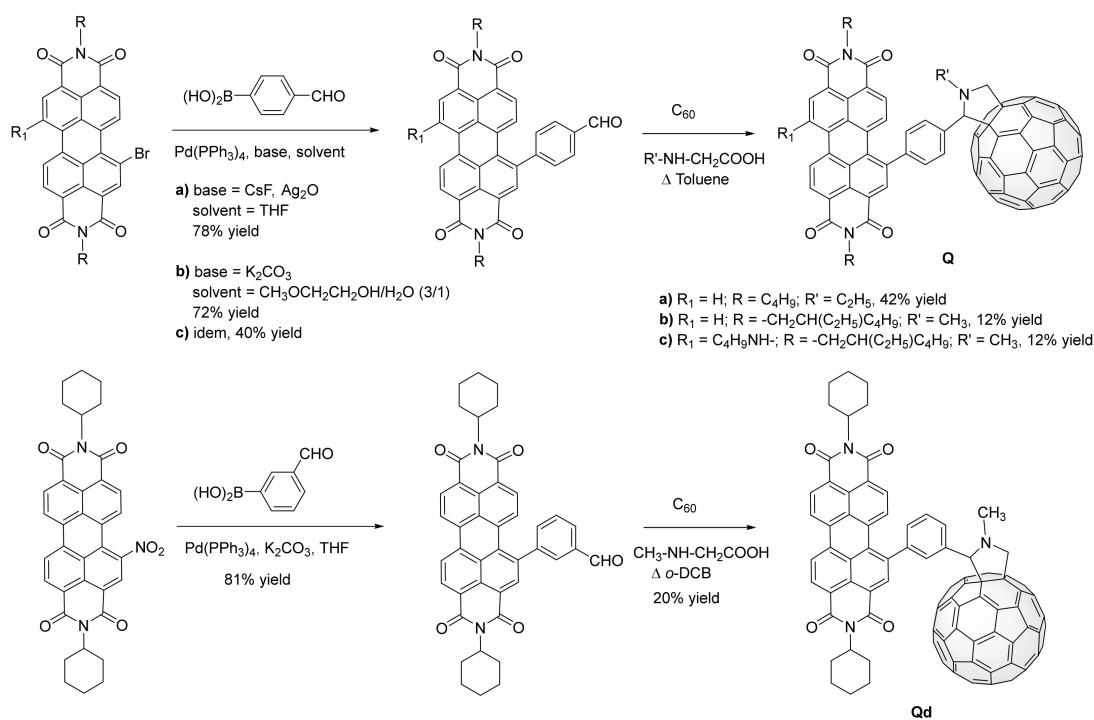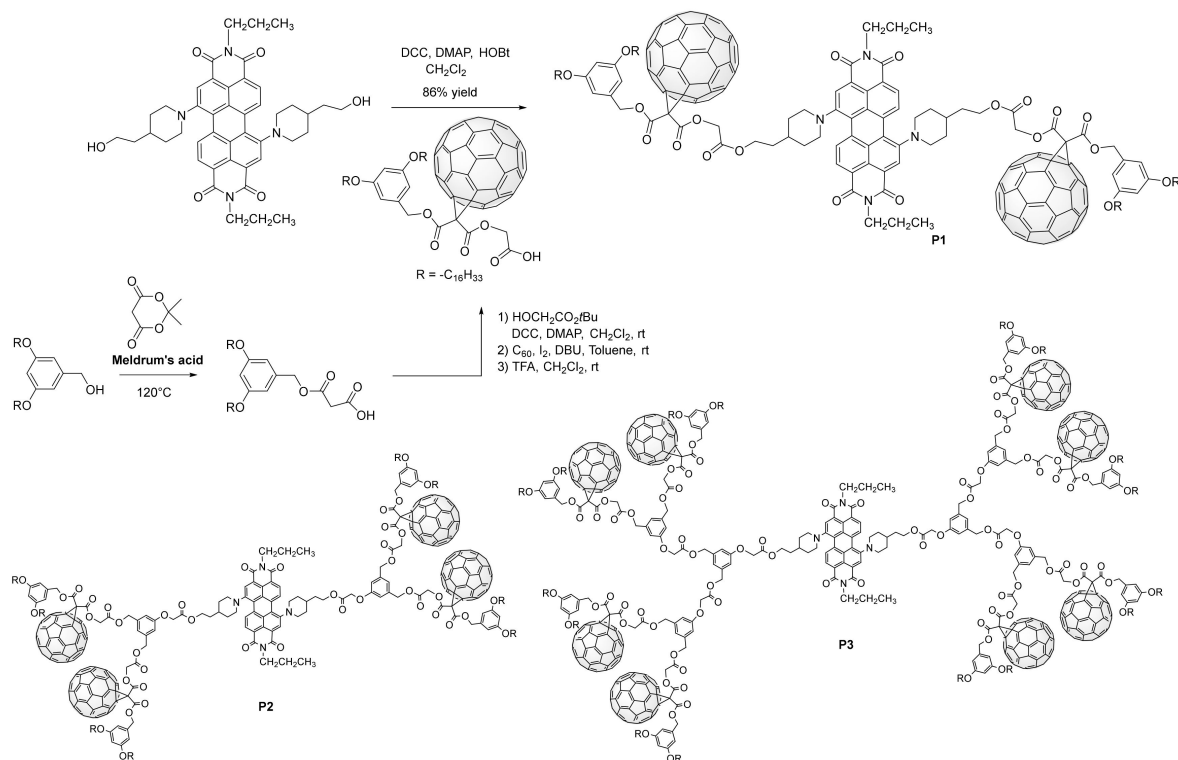
Scheme 8. Bay-PDI grafting of C_{60} derivative using aromatic nucleophilic substitution for dyads **Ma,b,c** and extension to the preparation of triads **Md,e** and conjugated polyacetylene **Mf** bearing PDI units and pendant C_{60} acceptors by D. Zhu and coll.
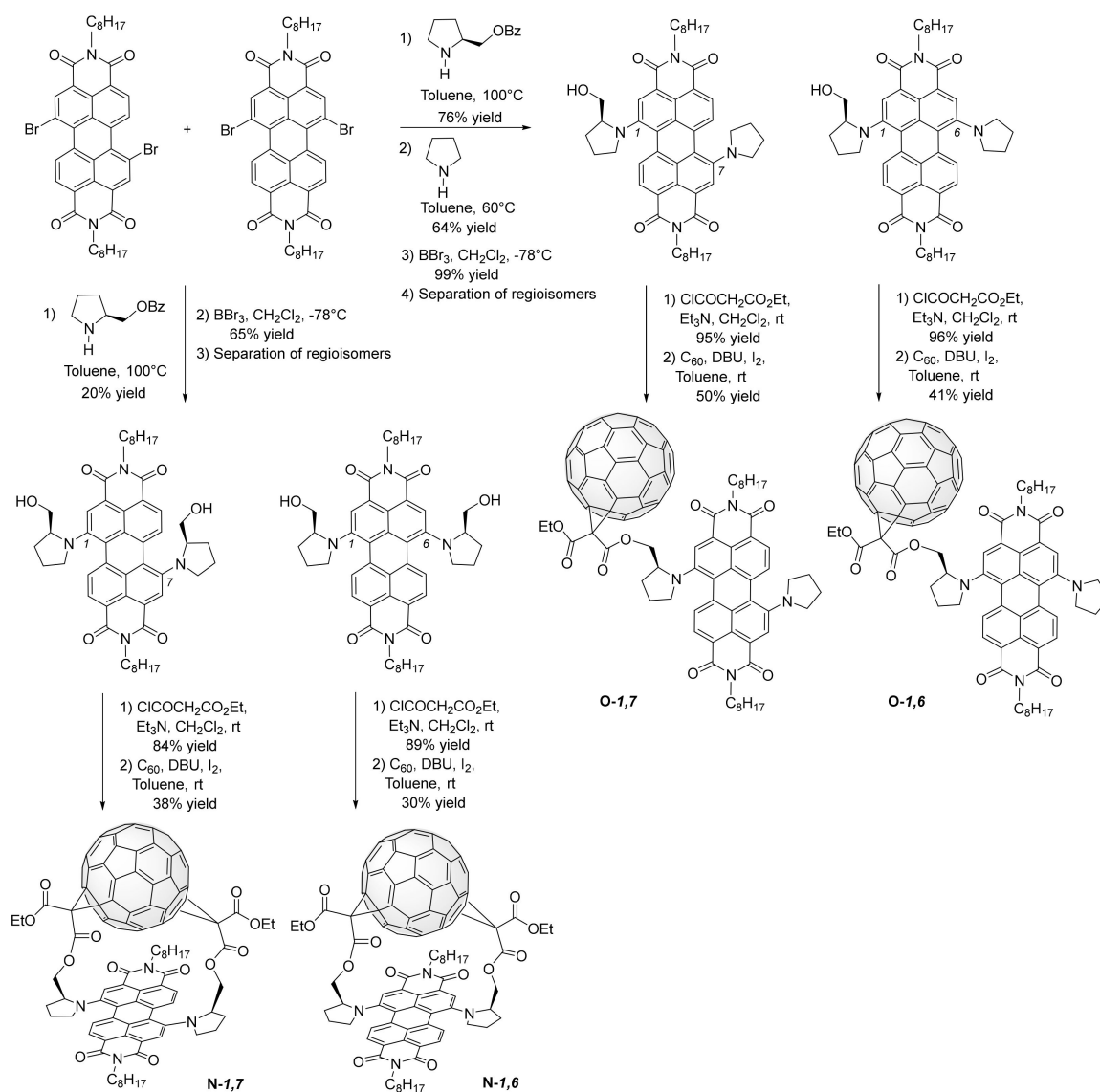
Scheme 9. Synthesis of 1,6 and 1,7-regioisomers of single and double-bridged pyrrolidino-substituted PDI-C$_{60}$ dyads **N** and **O**, respectively, by R.K. Dubey, H. Lemmetyinen and coll.

Bromination at the PDI bay position gives access to one of the most valuable starting materials which, especially through palladium-catalyzed Suzuki-Miyaura, Stille or Sonogashira coupling reactions allows the preparation of substituted PDIs by building carbon–carbon (C-C) single bonds. Thus, Suzuki–Miyaura coupling (SMC) and Prato reactions were combined for the synthesis of dyad **Qa** by N.R. Champness and coll. (Scheme 11) [84]. Starting from mono-bromoPDI, an SMC reaction using 4-formylphenyl boronic acid in the presence of CsF, Ag$_2$O, Pd(PPh$_3$)$_4$ in THF gave the corresponding aldehyde intermediate in 78% yield. Subsequent Prato reaction using C$_{60}$ and *N*-ethylglycine in refluxing toluene afforded dyad **Qa** in 42% yield. It should be noted that a mixture of 1,6/1,7-dibromoPDI was used to attain the corresponding triad C$_{60}$-PDI-C$_{60}$. J. Zhao and coll. described the synthesis of dyads **Qb** and **Qc** using a similar strategy and described their photophysical properties for use as singlet oxygen photosensitizers for photooxidation of 1,5-dihydroxynaphthalene [85]. More recently, our group has demonstrated the possibility to use mono-nitroPDI and bis-nitroPDI for creating C-C single bonds using the SMC coupling reaction [86–89], and consequently dyad **Qd** was prepared by this original strategy [90].

Scheme 10. Synthesis of dendritic branches **P₁₋₃** with peripheral fullerene subunits by J.-F. Nierengarten, N. Armaroli and coll.

Scheme 11. Suzuki–Miyaura coupling (SMC) and Prato reactions used for synthesis of dyad **Qa** by N. Champness and coll., dyads **Qb,c** by J. Zhao and coll. from bromoPDI, and dyad **Qd** by P. Hudhomme and coll. from nitroPDI.

3. Synthesis of a Platform for New C$_{60}$-PDI Assemblies

While different C$_{60}$-PDI dyads were developed in order to exploit their light-harvesting capabilities, to the best of our knowledge, no strategy has been investigated so far to introduce these chromophores onto a multifunctional platform allowing a post-functionalization. Consequently, we designed the 3-formyl-5-hydroxybenzoic acid as a platform incorporating functional groups for the introduction of both C$_{60}$ and PDI acceptors, and a free anchoring group that can be used for the attachment of an electron donor or otherwise a polymerizable group according to the intended application (Figure 2). The design of this platform with substituents in the 1,3,5 positions was justified to minimize steric hindrance and to avoid possible mesomeric effects between the different groups.
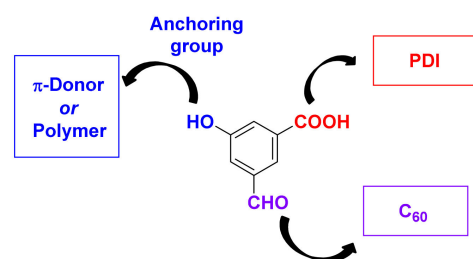
Figure 2. Presentation of the 3-formyl-5-hydroxybenzoic acid platform for incorporating C$_{60}$ using Prato reaction, PDI moiety by esterification and the free phenol anchoring group for the versatile attachment of an electron donor or a polymerizable group.

Building block 5-benzyloxy-3-formylbenzoic acid derivative **6** was synthesized in 6 steps in an overall 43% yield by improved modifications of a reported route (29% overall yield) for which experimental procedures were not described (Scheme 12) [91]. Esterification of commercially available 5-hydroxyisophthalic acid into diester **1** was followed by the protection of the phenol functionality into the benzyl group [92]. Monohydrolysis of resulting compound **2** using one equivalent of KOH in THF-MeOH [93] resulted after acidic treatment to key monoacid **3**. The selective reduction of the carboxylic group using the borane dimethylsulfide complex was followed by the oxidation step of primary alcohol **4** using PCC to obtain methyl 3-(benzyloxy)-5-formylbenzoate **5**. It is noteworthy to indicate that attempts for selective monoreduction of dimethyl isophthalate **2** into monoaldehyde **5** using DiBAl-H were unsuccessful. At last, treatment of compound **5** with LiOH in MeOH-H$_2$O followed by acidic work-up afforded targeted building block **6**.
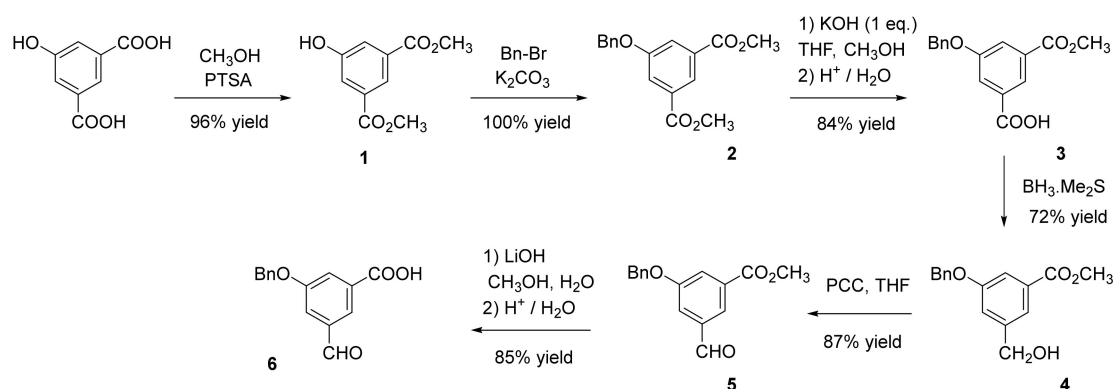

Scheme 12. Synthesis of the benzyl protected 3-formyl-5-hydroxybenzoic acid derivative.

Both PDI and C$_{60}$ units were grafted onto platform **6** by using the acid and formyl groups, respectively (Scheme 13). A Steglich type esterification [94] with PDI derivative **7**, prepared according to our previous report in 64% yield [48], and according to an esterification procedure, we have already experimented with fullerene chemistry [95], was achieved

affording compound **8** in 90% yield. The subsequent 1,3-dipolar cycloaddition reaction was carried out using C_{60} and sarcosine in refluxing toluene to give, after purification by silica gel column chromatography, dyad **9** in satisfying 60% yield. Several methods were investigated for the deprotection of the benzyl group. Whereas classical hydrogenation using H_2/Pd-C was unsuccessful, the reaction carried out using 47% solution HBr in the ionic liquid 1-butyl-3-methylimidazolium tetrafluoroborate (BMIM-BF$_4$) [96] afforded dyad **10** in 21% yield. The best result was obtained by treating compound **9** with a solution of BCl$_3$ [97] in CH$_2$Cl$_2$ at -78 °C leading to dyad **10** in 70% yield.

Dyads **9** and **10** were characterized by ^{1}H and ^{13}C NMR, MALDI-TOF mass spectrometry and for dyad **10** 2D-NMR analyses consisting of COSY, HMQC, and HMBC experiments were investigated (see Supplementary Materials). For dyad **9**, variable temperature NMR spectra recorded in CDCl$_3$ showed a modification of the shape of one of the two characteristic perylene singlet signals when the temperature was increased to 328 K. Indeed, the ^{1}H NMR spectrum at 298 K of dyad **10** showed for the perylene protons a well-defined singlet for two protons and a broad singlet for the two others. When recorded at 328 K, the two expected singlets at 8.20 and 8.24 ppm were correctly observed. Concerning the three protons of the aromatic platform, only one of these protons at 7.38 ppm was observed in the spectrum at 298 K. This phenomenon could result from the presence of both fullerene and PDI substituents around this aromatic platform. On the contrary, the spectrum recorded at 328 K showed a well-defined doublet of doublet at 7.40 ppm (^3J = 1.5 and 2.4 Hz) accompanied by two broad singlets at 7.47 and 7.83 ppm. It is reasonable to consider that both protons correspond to those which are closer to bulky C_{60}.
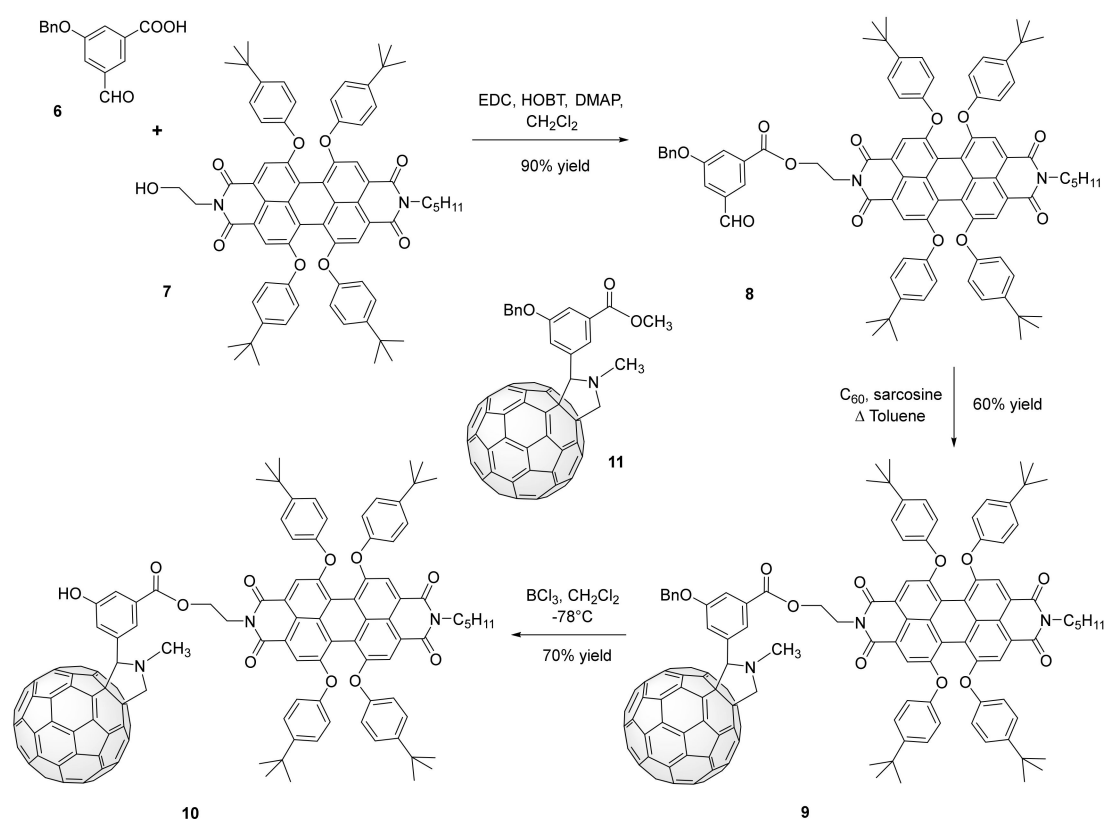

Scheme 13. Synthesis of C_{60}-PDI dyad **10**.

Electrochemical properties of dyad **9**, PDI **8**, and fulleropyrrolidine (FP) **11** references were analyzed by cyclic voltammetry in CH$_2$Cl$_2$ (or a mixture with CS$_2$ in the case of compound **11**), in *n*-Bu$_4$NPF$_6$ 0.1 M solution as the supporting electrolyte (Table 1). The voltammograms have been deconvoluted in order to obtain the number of electrons in-

volved in the processes. Dyad **9** showed three reversible reduction waves (Figure 3). The first two-electron process at E^o_{red1} = −1.22 V (vs Fc$^+$/Fc) was assigned to the formation of the $C_{60}{}^{-\cdot}$-PDI$^{-\cdot}$ species. This process suggests that the first reduction wave of fullerene and the first reduction wave of the PDI are overlapping. This observation confirms that the type of linkage functionality onto C_{60} and between the two electroactive units slightly influences the redox potentials. Indeed, we have previously shown that, for the same substituted PDI derivative but anchored to a methanofullerene using an aliphatic linkage, four distinguishable reduction waves were observed [45,46]. In that case, the first reduction wave was attributed to the $C_{60}{}^{-\cdot}$-PDI species with 0.14 V of difference with the second reduction attributed to the $C_{60}{}^{-\cdot}$-PDI$^{-\cdot}$ species. The second one-electron reduction process of dyad **9** corresponding to the formation of the $C_{60}{}^{-\cdot}$-PDI^{2-} species was at E^o_{red2} = −1.38 V. The third one-electron reduction wave appearing at E^o_{red3} = −1.55 V resulted from the formation of $C_{60}{}^{2-}$-PDI^{2-}. A first reversible two-electron oxidation process arises at E^o_{ox1} = +0.81 V. Moreover, comparison of these different values for dyad **9** with reference compounds **8** and **11** suggests that there is no significant interaction taking place between both electroactive moieties in the ground state.

(a)

(b)
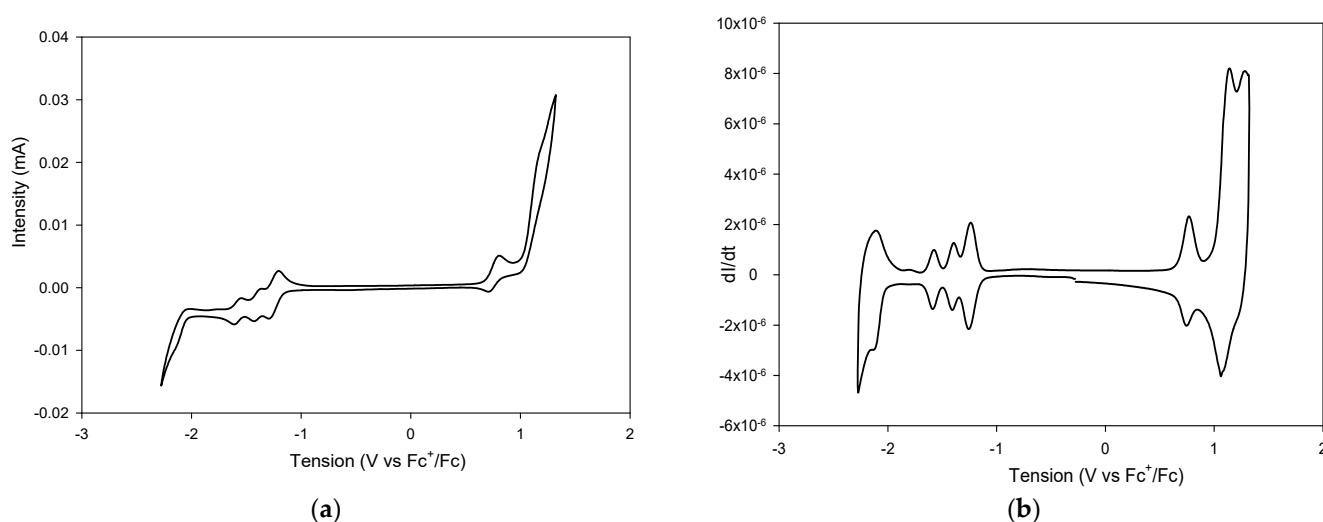
Figure 3. Cyclic voltammogram (**a**) and deconvoluted cyclic voltammogram (**b**) of dyad C_{60}-PDI **9** (C = 5 × 10^{-4} M), Pt electrodes, CH_2Cl_2/*n*-Bu$_4$NPF$_6$ (0.1 M).

Table 1. Oxidation and reduction potentials of dyad **9**, references PDI **8**, and fullerene **11**. (V vs. Fc$^+$/Fc). Scan rate: 100 mV/s.

Compound	E^0_{red3}	E^0_{red2}	E^0_{red1}	E^0_{ox1}
PDI **8**	-	−1.40	−1.24	+0.77
Dyad **9**	−1.55	−1.38	−1.22 *	+0.81 *
FP **11**	−1.78	−1.55	−1.18	+0.98 **

* Two-electrons reduction or oxidation process; ** irreversible process.

The optical properties of PDI **7** and dyad **9** were analyzed in CH_2Cl_2 solutions by UV-vis absorption (*ca.* 10^{-5} M) and photoluminescence emission (*ca.* 5 × 10^{-6} M) spectroscopy (see Supplementary Materials). Reference PDI **7** and dyad **9** are characterized by the three characteristic absorption bands of the PDI core at around 450, 540, and 580 nm, and the maximum absorption of dyad **9** at 229 nm is ascribed to the fullerene moiety. The UV–vis spectrum of PDI-C_{60} dyad **9** corresponds to the linear combination of PDI and C_{60} absorption spectra suggesting the absence of electronic coupling in the ground state between the PDI and fullerene moieties. A quasi-quantitative quenching of fluorescence was observed for dyad **9**, due to the strong interaction, probably energy transfer according

to results on our previous reported systems [46,49], between the PDI and C_{60} in the excited state (Table 2).

Table 2. Absorption spectra in CH_2Cl_2 and toluene for PDI **7** and dyad **9** (C = 10^{-5} M): λ_{max} is underlined. Emission spectra in CH_2Cl_2 and toluene for PDI **7** and dyad **9** (λ_{exc} = 520 nm; C = 5×10^{-6} M): quantum yields were calculated using cresyl violet perchlorate as reference (φ_F = 0.54 in ethanol).

Compound	λ_{abs} (nm) (CH_2Cl_2)	λ_{abs} (nm) (toluene)	λ_{em} (nm) (CH_2Cl_2)	λ_{em} (nm) (toluene)	φ_F (CH_2Cl_2)	φ_F (Toluene)
PDI **7**	452, 540, 580	448, 535, 575	607	601	~1	~1
Dyad **9**	229, 452, 543, 579	283, 451, 535, 573	610	603	2.8×10^{-3}	1.1×10^{-2}

We propose here a new polymeric architecture involving together PDI and C_{60} units on a non-conductive side-chain polymethacrylate in which C_{60}-PDI dyads are attached as pendant moieties onto the main chain of the polymer. From the literature, with the aim of fabricating well-ordered nanostructured BHJ photovoltaic devices presenting a large donor/acceptor interface in an all-polymers strategy, M. Thelakkat and coll. have synthesized unsymmetrical poly(PDI-acrylate) (PPDI-Acr) [98] and a series of PPDI-Acr-based diblock copolymers [99–102]. The PDI-Acr monomer was also used as a building block to prepare polymers and donor–acceptor diblock copolymers with PDI pendant groups for applications in organic field-effect transistors (OFETs) [103–105]. Poly(methacrylate)s labeled with PDI derivatives were also described as long-wavelength absorbing dyes [106]. It should be noted that pendant PDI-*tert*-butyl acrylate copolymers have shown efficient energy transfer within PDI luminophores in the polymer suggesting potential use in luminescent solar concentrators [107]. Concerning the C_{60} counterpart, only a few poly(methyl methacrylates) containing covalently attached fullerene C_{60} were synthesized [108–110]. In particular, it was shown that the fullerene attached to the branched poly(methyl methacrylate) could act as an inhibitor of the cross-linking radical polymerization of dimethacrylate.

To demonstrate the ability of the phenolic group of platform **6** to be functionalized, the reaction of dyad **10** with methacryloyl chloride was successfully carried out in the presence of triethylamine and 4-dimethylaminopyridine (DMAP) in CH_2Cl_2 (Scheme 14). This result clearly demonstrated that the steric hindrance suspected around the platform due to the presence of both C_{60} and PDI was not a limiting factor to a post-functionalization process. This dyad **12** was characterized by ^{1}H and ^{13}C NMR and exhibited the molecular peak at m/z = 2059 by MALDI-TOF mass spectrometry.

For the synthesis of polymer 3 (**Pol 3**), we have opted for an addition-elimination reaction carried out on dyad **10** with commercial poly(methacryloyl chloride) (25% solution in dioxane, Polyscience) in dry dioxane in the presence of triethylamine. Indeed, although a co-polymerization of dyad **12** and methyl methacrylate could be considered [111], C_{60} acting as a radical scavenger during the free-radical polymerization [112], we thought that homopolymerization of dyad **12** could be difficult to occur due to the volume of the substituent of the methacrylate unit which determines the penultimate-unit effect during the free-radical polymerization or co-polymerization process [113].

Two other polymers were prepared as references, starting from PDI derivative **7** and *tert*-butylphenol giving **Pol 2** and **Pol 1**, respectively. Characterization by IR spectroscopy of the obtained polymers showed the total disappearance of the ν_{OH} vibration band of the aliphatic alcohol or phenolic function of starting materials. The characteristic signals of the ester vibrations $\nu_{C=O}$ = 1748 cm^{-1} and ν_{C-O} = 1204–1014 cm^{-1} were shown for reference polymer **Pol 1**. These vibration bands $\nu_{C=O}$ = 1759 cm^{-1} (ester) and ν_{C-O} = 1340–1100 cm^{-1} were also observed for **Pol 2** and **Pol 3**, with the additional vibration band at $\nu_{C=O}$ = 1654 cm^{-1} of the imide groups arising from the PDI skeleton.
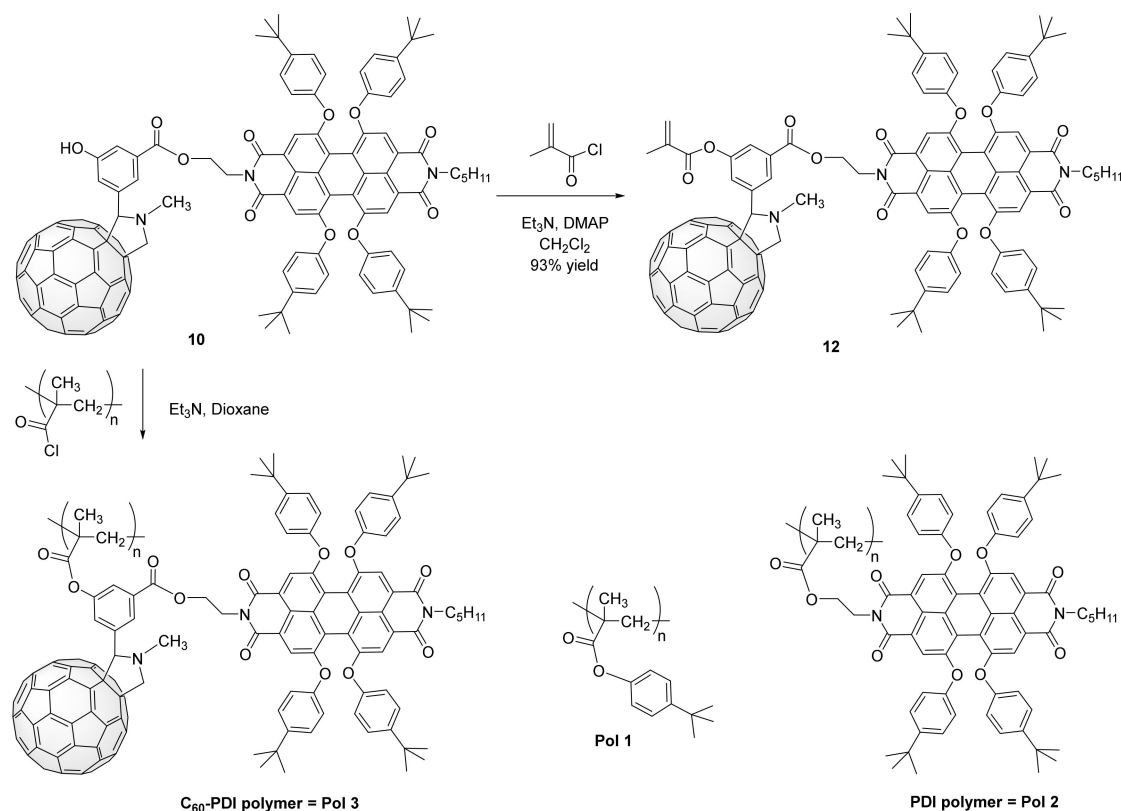
Scheme 14. Synthesis of dyad **12**, C_{60}-PDI polymer **Pol 3**, and PDI-based polymer **Pol 2**, *tert*-butylphenol based polymer **Pol 1** for references.

Differential scanning calorimetry (DSC) was used for the determination of the glass transition temperature (T_g) value of C_{60}-PDI polymer **Pol 3** which is equal to 151 °C. This has to be compared with the T_g values of 59 °C and 105 °C for **Pol 1** and poly(methyl methacrylate) (PMMA), respectively. This higher T_g value can be explained by several interconnected factors such as the steric hindrance which could reduce the degree of substitution on the polymeric chain. Moreover, unreacted acyl chloride groups also undergo some hydrolysis in acid groups which leads to an increase in the T_g as a result of hydrogen bond interaction that reduces the mobility. Moreover, although the substituent corresponding to dyad **10** represents a bulky group, it can also form aggregates due to π-π stacking interactions which limit the mobility of the polymer segment chains, thus explaining the higher T_g value of **Pol 3** compared to PMMA. Moreover, the thermogravimetric analysis (TGA) clearly showed the higher stability of **Pol 3** composed of both PDI and C_{60} units (Figure 4).

The concentration of dye vs. dyad in the polymer samples was determined using a colorimetric technique employing Lambert Beers' law. A calibration curve was obtained by plotting the absorbance against the concentration of dye solutions of known concentrations. The technique allowed the determination of a 73% (weight ratio, 18% molar ratio) content of perylene dye in the PDI polymer **Pol 2** used as a reference sample. The same approach was applied for C_{60}-PDI dyad polymer **Pol 1** resulting in a 62% weight ratio, with a 6.5% molar ratio of dyad content (see Supplementary Materials).
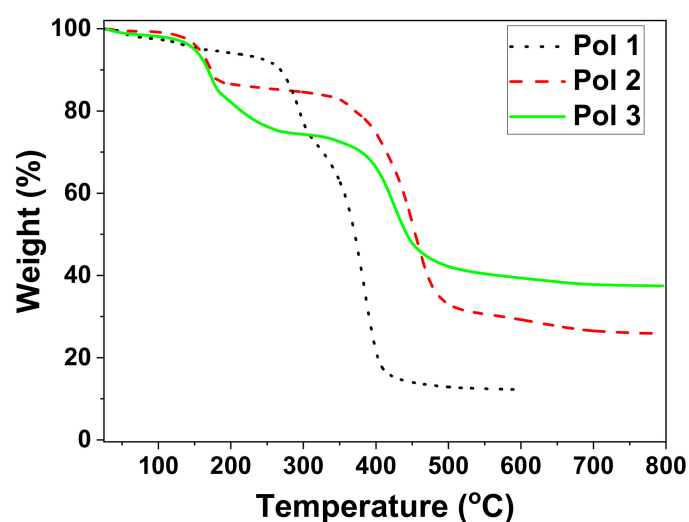
Figure 4. TGA spectra of **Pol 1** (dotted line), **Pol 2** (dashed line) and **Pol 3** (full line) recorded by a heating rate of 10 °C min^{-1} under N_2 atmosphere.

4. Conclusions

In conclusion, our first objective was to establish the state-of-the-art of the different synthetic methodologies described to date to prepare C_{60} and PDI-based assemblies focusing on the two possibilities for attachment of C_{60} on the imide or bay PDI positions. Secondly, we report here a straightforward and versatile method to prepare an aromatic platform bearing three different phenol, aldehyde, and carboxylic acid functional anchors. This platform was employed for the attachment of C_{60} and PDI dye and then took advantage of the free phenol function to prepare original methacrylate monomer and pendant poly(methacrylate) macromolecules. A complete and detailed investigation of the photophysical properties of this polymer is currently in progress. This synthetic approach appears very promising for the preparation of different triads since functionalities such as π-donors for example can be introduced on the phenolic anchor site in the last synthetic step.

5. Experimental Procedures

Dimethyl 5-hydroxyisophthalate 1:

A solution of commercial 5-hydroxyisophthalic acid (6.34 g, 0.035 mol) and *p*-toluenesulfonic acid (1.21 g, 0.007 mol) in methanol (120 mL) was stirred at reflux for 24 h. The solvent was partially removed in vacuo and after the addition of diethyl ether, the solution was neutralized using an aqueous sodium hydroxide solution. The resulting organic layer was washed with water, dried over $MgSO_4$, then concentrated in vacuo. The product (6.97 g) was obtained as a white powder in 96% yield. Spectroscopic data are in agreement with the literature [92]. ^{1}H NMR (acetone-d_6, 300 MHz) δ: 9.20 (s, 1H, OH), 8.10 (t, J = 1.5 Hz, 1H, PhH), 7.68 (d, J = 1.5 Hz, 2H, PhH), 3.90 ppm (s, 6H, OCH$_3$).

Dimethyl 5-(benzyloxy)isophthalate 2:

A solution of dimethyl 5-hydroxyisophthalate **1** (5.8 g, 0.027 mol) and K_2CO_3 (5.7 g, 0.041 mol) in anhydrous acetone (120 mL) was degassed with N_2 before the addition of benzyl bromide (3.4 mL, 0.027 mol). The reaction mixture was stirred at reflux under N_2 for 24 h. Acetone was removed in vacuo and the remaining solid was dissolved in ethyl acetate and then washed with water. The aqueous layer was extracted with ethyl acetate, and the organic layer was washed with brine, dried over $MgSO_4$, and concentrated in vacuo to give compound **2** as a white solid (8.25 g, 100%). Spectroscopic data are in agreement with the literature [92,93]. ^{1}H NMR (acetone-d_6, 300 MHz) δ: 8.20 (t, J = 1.5 Hz, 1H, PhH), 7.83 (d, J = 1.5 Hz, 2H, PhH), 7.55–7.35 (m, 5H, OPhH), 5.28 (s, 2H, OCH$_2$), 3.92 ppm (s, 6H, OCH$_3$).

3-(Benzyloxy)-5-(methoxycarbonyl) benzoic acid 3:

Potassium hydroxide, 85% in pellets (0.84 g, 0.013 mol) was added to a solution of dimethyl 5-(benzyloxy)isophthalate **2** (4 g, 0.013 mol) in a mixture of methanol (60 mL) and

THF (30 mL). The reaction mixture was stirred at reflux under N_2 overnight. The solvent was removed in vacuo, and the remaining slurry was dissolved in water and washed with CH_2Cl_2. Concentrated HCl was added to the aqueous layer to reach pH = 3. The resulting white precipitate was collected by vacuum filtration and dried to give compound **3** as a white solid (3.2 g, 84%). Spectroscopic data are in agreement with the literature [92]. ^{1}H NMR (acetone-d_6, 300 MHz) δ: 8.24 (m, 1H, PhH), 7.86 (m, 1H, PhH), 7.86 (m, 1H, PhH), 7.83 (m, 1H, PhH), 7.55–7.34 (m, 5H, OPhH), 5.28 (s, 2H, OCH$_2$), 3.92 (s, 3H, OCH$_3$).

Methyl 3-(benzyloxy)-5-(hydroxymethyl)benzoate 4:

$BH_3(CH_3)_2S$ complex (2.0 M in THF, 4.2 mL, 8 mmol) was added dropwise to a solution of compound **3** (2 g, 7 mmol) in anhydrous THF (25 mL) at 0 °C. The mixture was then stirred at reflux overnight. The reaction was quenched and neutralized by the addition of an H_2O/CH_3COOH (1:2) solution (6 mL). The solvents were removed in vacuo and the slurry was dissolved in ethyl acetate, washed successively with a 30% K_2CO_3 aqueous solution, then 1N HCl aqueous solution, saturated $NaHCO_3$ aqueous solution, and brine. After drying over anhydrous Na_2SO_4, the solution was then concentrated. The product was purified by silica gel column chromatography using petroleum ether and ethyl acetate (4:1) as the mixture of eluents. The product was obtained as colorless oil (1.36 g, 72%) which crystallized by freezing. Spectroscopic data are in agreement with the literature [92]. ^{1}H NMR (acetone-d_6, 300 MHz) δ: 7.62 (m, 1H, PhH), 7.52–7.28 (m, 7H, PhH), 5.18 (s, 2H, OCH$_2$), 4.68 (d, J = 5.7 Hz, 2H, OCH$_2$), 4.40 (t, J = 5.7 Hz, 1H, OH), 3.86 (s, 3H, OCH$_3$).

Methyl 3-(benzyloxy)-5-formylbenzoate 5:

A solution of pyridinium chlorochromate (2.77 g, 0.013 mol) in THF (25 mL) was added to a solution of compound **4** (2.8 g, 0.011 mol) in THF (25 mL). The reaction mixture was heated at reflux for 24 h. After dilution with CH_2Cl_2 (30 mL), the solution was filtered through celite, washed with a saturated NH_4Cl solution and water, dried over $MgSO_4$, and concentrated in vacuo. The residue was purified by silica gel column chromatography using petroleum ether and ethyl acetate (4:1) as the mixture of eluents and compound **5** was isolated as a white precipitate (2.41 g, 87%). Spectroscopic data are in agreement with the literature [92]. ^{1}H NMR (acetone-d_6, 300 MHz) δ: 10.09 (s, 1H, CHO), 8.12 (t, J = 1.5 Hz 1H, PhH), 7.88 (dd, J = 1.2 Hz and 1.5 Hz, 1H, PhH), 7.77 (dd, J = 1.2 Hz and 1.5 Hz, 1H, PhH), 7.55–7.35 (m, 5H, PhH), 5.31 (s, 2H, OCH$_2$), 3.93 ppm (s, 3H, OCH$_3$).

3-(Benzyloxy)-5-formylbenzoic acid 6:

To a solution of compound **5** (0.6 g, 2.2 mmol) in methanol and water (48 mL, 3:1) was added lithium hydroxide (0.1 g, 4.4 mmol). The mixture was stirred at room temperature overnight and most of the methanol was removed in vacuo. The aqueous solution was diluted and washed with CH_2Cl_2. The solution was acidified until pH = 3 using an HCl aqueous solution. The precipitate was collected by filtration and dried to give compound **6** as a white solid (0.48 g, 85%). Spectroscopic data are in agreement with the literature [92]. ^{1}H NMR (acetone-d_6, 300 MHz) δ: 10.09 (s, 1H, CHO), 8.15 (t, J = 1.5 Hz, 1H, PhH), 7.91 (dd, J = 1.5 Hz and 2.7 Hz, 1H, PhH), 7.77 (dd, J = 1.5 Hz and 2.7 Hz, 1H, PhH), 7.56–7.35 (m, 5H, PhH), 5.31 (s, 2H, OCH$_2$). ^{13}C NMR (Acetone-d_6, 75 MHz) δ:193.2; 167.4; 161.4; 140.3; 138.6; 134.9; 130.4; 129.9; 129.6; 125.3; 123.41; 120.1; 72.1.

*Compound **7**:*

A mixture of *N*-2′-Hydroxyethyl-*N*′-pentyl-1,6,7,12-tetrakischloroperylene- 3,4:9,10-*bis*(dicarboximide) [48] (860 mg, 1.4 mmol), *p*-tertiobutylphenol (2.1 g, 14 mmol) and K_2CO_3 (2 g, 14.5 mmol) in anhydrous *N*-methylpyrrolidone (NMP) (50 mL) was stirred at 130 °C under argon for 14 h. After being cooled to room temperature, the reaction mixture was poured into HCl solution (1N) (50 mL). The precipitate was collected by filtration, washed thoroughly with water until neutrality, and then purified by column chromatography on silica gel using successively CH_2Cl_2 and then CH_2Cl_2/acetone (30:1) as the mixture of eluents. Crystallization from CH_2Cl_2/methanol afforded compound **7** as a purple powder which was dried overnight in vacuum at 80 °C (975 mg, 64% yield). ^{1}H NMR (CDCl$_3$, 300 MHz) δ: 8.26 (s, 2H), 8.24 (s, 2H), 7.28–7.23 (m, 8H), 6.86–6.83 (m, 8H), 4.41 (t, ^3J = 7 Hz, 2H), 4.12 (broad t, ^3J = 7 Hz, 2H), 3.95 (t, ^3J = 7 Hz, 2H), 2.2 (broad s, 1H), 1.70 (broad t, 2H),

1.40–1.35 (m, 4H), 1.31 (s, 36H), 0.90 (t, ^3J = 7 Hz, 3H). ^{13}C NMR (75 MHz, CDCl$_3$) δ 164.4, 163.6, 156.3, 156.0, 153.0, 152.9, 147.5, 147.4, 133.1, 133.0, 126.8, 122.8, 122.1, 121.1, 120.4, 119.9, 119.7, 119.5, 119.4, 77.4, 61.9, 43.0, 40.8, 34.5, 31.6, 29.3, 27.9, 22.5, 14.1.

Compound **8**:

To a degassed solution of 3-(benzyloxy)-5-formylbenzoic acid **6** (100 mg, 0.390 mmol) in anhydrous CH$_2$Cl$_2$ (30 mL) was added hydroxybenzotriazole (HOBt) (53 mg, 0.390 mmol), *N*-(3-dimethylaminopropyl)-*N'*-carbodiimide (EDC) (82 µL, 0.429 mmol), 4-dimethylamino-pyridine (48 mg, 0.39 mmol) and compound **7** (428 mg, 0.39 mmol). The mixture was stirred at room temperature under argon for 5 days. The solvent was removed under reduced pressure and the residue was purified by silica gel column chromatography using CH$_2$Cl$_2$/acetone (30:1) as the mixture of solvents. Compound **8** was isolated as a purple powder (470 mg, 90%). ^{1}H NMR (CDCl$_3$, 500 MHz) δ: 9.89 (s, 1H), 8.23 (s, 2H), 8.20 (s, 2H), 7.99 (t, *J* = 1.5 Hz, 1H), 7.83 (dd, *J* = 1.5 Hz and 2.7 Hz, 1H, PhH), 7.61 (dd, *J* = 1.5 Hz and 2.7 Hz, 1H, PhH), 7.38–7.28 (m, 5H), 7.24 and 7.23 (2d, *J* = 9 Hz, 8H), 6.82 and 6.81 (2d, *J* = 8.7 Hz, 8H), 5.07 (s, 2H), 4.66–4.55 (br t, 4H), 4.12–4.07 (br t, 2H), 1.66 (br t, 2H), 1.35 (m, 4H), 1.29 (s, 18H), 1.28 (s, 18H), 0.87 (t, *J* = 7.2 Hz, 3H). ^{13}C NMR (CDCl3, 125 MHz) δ:191.0; 165.1; 163.5; 163.4; 159.2; 156.1; 155.8; 152.9; 152.7; 147.3; 147.2; 137.8; 135.8; 133.0; 132.8; 128.6; 128.2; 127.5; 126.7; 122.6; 122.0; 121.0; 120.2; 119.4; 119.1; 77.2; 70.4; 34.6; 34.4; 31.4; 31.6; 29.2; 22.4; 13.9. MS (MALDI-TOF, pos. mode, dithranol): *m/z*: calcd for: 1334.59; found: 1334.6 [M]$^+$ HRMS (ESI FAB+): calcd for C$_{86}$H$_{82}$N$_2$O$_{12}$: 1334.586777; found: 1334.5865. Elemental analysis for C$_{86}$H$_{82}$N$_2$O$_{12}$ (1335.58) calcd. C 77.34 H 6.19 N 2.10; found C 77.13, H 6.40, N 2.00.

Dyad **9**:

To a solution of compound **8** (250 mg, 0.18 mmol) in anhydrous toluene (70 mL) were added C$_{60}$ (200 mg, 0.27 mmol) and N-methylglycine (sarcosine) (60 mg, 0.67 mmol). The reaction mixture was refluxed under nitrogen for 24 h. After the solution was cooled to room temperature, the solvent was removed under reduced pressure and the residue was purified by silica gel column chromatography using CS$_2$ as the eluent to remove the excess C$_{60}$ with CS$_2$, then toluene/ethyl acetate (100:1) as the mixture of solvents. Dyad **9** was isolated as a purple powder (225 mg, 60%). ^{1}H NMR (CDCl$_3$, 500 MHz, 298 K) δ: 8.26 (br s, 2H), 8.19 (s, 2H), 7.58 (br s, 1H), 7.38–7.28 (m, 4H), 7.21–7.17 (m,10H), 6.77 (m, 8H), 5.05 (br s, 2H), 4.90 (d, *J* = 10 Hz, 1H), 4.77 (s, 1H), 4.62 (br s, 2H), 4.41 (br s, 1H), 4.16 (br s, 1H), 4.12 (br t, 2H), 2.67 (s, 3H), 1.70 (br t, 2H), 1.35 (m, 4H), 1.27 (s, 18H), 1.26 (s, 18H), 0.89 (t, 3H). At 298 K, the signal corresponding to two protons of the PDI at 8.26 ppm is not well resolved. A temperature-dependent NMR experiment showed perfectly the singlet at 328 K. ^{1}H NMR (CDCl$_3$, 500 MHz, 328 K): δ = 8.26 (s, 2H), δ = 8.19 (s, 2H). ^{13}C NMR (CDCl$_3$, 125 MHz) δ: 166.2, 163.6, 163.5, 156.3, 155.6, 153.3, 153.0, 147.4, 147.3, 147.2, 146.4, 146.1, 146.0, 145.8, 145.4, 145.3, 145.1, 144.4, 142.7, 142.6, 142.2, 142.1, 142.0, 141.7, 139.4, 136.7, 136.5, 135.7, 133.1, 128.7, 128.2, 127.7, 126.8, 126.7, 122.7, 122.1, 121.5, 120.8, 120.6, 120.0, 119.5, 119.2, 83.0, 74.0, 70.0, 69.0, 40.8, 40.0, 34.5, 31.6, 29.4, 28.0, 22.6, 14.1. MS (MALDI-TOF, pos. mode, dithranol): *m/z*: calcd for: 2081.53; found: 2082.5 [M]$^+$ HRMS (ESI FAB+): calcd for C$_{148}$H$_{87}$N$_3$O$_{11}$: 2081.634062; found: 2082.6468. Elemental analysis for C$_{148}$H$_{87}$N$_3$O$_{11}$ (2083.29) calcd. C 85.33 H 4.21 N 2.02; found C 82.99, H 4.27, N 1.98.
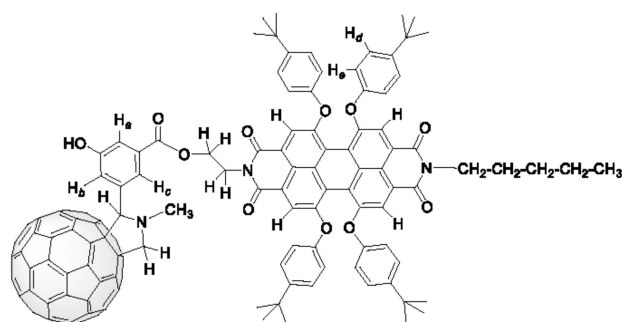
Dyad **10**:

Experimental procedure using HBr/BMIM-BF$_4$:

Dyad **9** (100 mg, 0.048 mmol) and concentrated hydrobromic acid (47%, 0.96 mmol) in 1-*n*-butyl-3-methylimidazolium tetrafluoroborate (BMIM-BF$_4$) (1.5 mL) were stirred at 115 °C for 36 h. The reaction mixture was extracted with CH$_2$Cl$_2$, washed with water, dried on MgSO$_4$, and concentrated in vacuo. Purification of the residue by silica gel column chromatography using CH$_2$Cl$_2$/acetone (30:1) as the mixture of solvents furnished a purple powder (20 mg, 21%).

Experimental procedure using BCl$_3$:

To a solution of dyad **9** (372 mg, 0,179 mmol) in anhydrous CH$_2$Cl$_2$ (40 mL), cooled to −78 °C under argon, was added BCl$_3$ 1M in CH$_2$Cl$_2$ (3.5 mL). After stirring at −78 °C

for 2 h, methanol (1 mL) was slowly added and the temperature was left to reach room temperature. The solvent was removed under reduced pressure and this cycle of methanol addition and evaporation was repeated 3 times. The mixture was then neutralized with 28% ammonia solution. After extraction with CH_2Cl_2 and concentration in vacuo, the residue was purified by silica gel column chromatography using CH_2Cl_2/acetone 30:1 as the mixture of solvents. Dyad **10** was precipitated using CH_2Cl_2/Petroleum ether and isolated as a purple powder (250 mg, 70%). ^{1}H NMR (CDCl$_3$, 500 MHz, 298 K) δ: 8.21 (br s, 2H, H perylene), 8.19 (s, 2H, H perylene), 7.39 (br s, 1H, Ha or Hb or Hc), 7.20 and 7.19 (2d, ^3J = 8.5 Hz, 8H, H$_D$ or H$_E$), 6.78 and 6.76 (2d, ^3J = 8.5 Hz, 8H, H$_D$ or H$_E$), 6.03 (br s, 1H, OH), 4.88 (d, J = 9.5 Hz, 1H, -NCH$_2$CH$_2$O-), 4.76 (s, 1H, CH pyrrolidine), 4.69 (br s, 1H, -NCH$_2$CH$_2$O-), 4.58 (br s, 2H, CH$_2$ pyrrolidine), 4.45 (br s, 1H, -NCH$_2$CH$_2$O-), 4.16 (br s, 1H, -NCH$_2$CH$_2$O-), 4.10 (t, J = 7.5 Hz, 2H, $\underline{NCH_2}$(CH$_2$)$_3$CH$_3$), 2.68 (s, 3H, N-CH$_3$), 1.67 (m, 2H, -CH$_2$-), 1.37 (m, 4H, -CH$_2$CH$_2$-), 1.28 (s, 36H, *t*Bu), 0.90 (t, J = 7 Hz, 3H, CH$_3$).

Two protons of the aromatic platform were not characterized on the spectrum at 298 K. This problem was solved by recording the ^{1}H NMR spectrum at 328 K. ^{1}H NMR (CDCl$_3$, 300 MHz, 328 K) δ: 8.24 (s, 2H, H perylene), 8.20 (s, 2H, H perylene), 7.83 (br s, 1H, Ha or Hb or Hc), 7.47 (br s, 1H, Ha or Hb or Hc), 7.40 (dd, 1H, ^3J = 1.5 and 2.4 Hz, Ha or Hb or Hc), 7.21 (d, ^3J = 9 Hz, 8H, H$_D$ or H$_E$), 6.78 and 6.81 (2d, ^3J = 9 Hz, 8H, H$_D$ or H$_E$), 5.57 (br s, 1H, OH), 4.89 (d, J = 9.3 Hz, 1H), 4.78 (s, 1H, CH pyrrolidine), 4.60 (m, 4H), 4.14 (m, 3H), 2.68 (s, 3H, N-CH$_3$), 1.71 (m, 2H, -CH$_2$-), 1.39 (m, 4H, -CH$_2$CH$_2$), 1.29 and 1.30 (2s, 36H, *t*Bu), 0.91 (t, J = 7 Hz, 3H, CH$_3$) (Figure 5). ^{13}C NMR (CDCl$_3$, 75 MHz) δ: 165.9, 163.5, 163.4, 156.1, 155.7, 155.6, 153.0, 152.8, 147.2, 147.1, 146.2, 146.1, 146.0, 145.9, 145.8, 145.7, 145.6, 145.5, 145.3, 145.2, 145.1, 144.9, 144.4, 144.3, 144.2, 143.9, 142.7, 142.5, 142.4, 142.2, 142.1, 142.0, 141.9, 141.8, 141.75, 141.70, 141.6, 141.5, 141.4, 141.2, 139.9, 139.5, 139.2, 139.1, 136.6, 136.1, 135.6, 132.9, 132.8, 126.6, 122.5, 121.8, 121.3, 120.4, 120.3, 119.9, 119.6, 119.3, 119.1, 82.7, 69.8, 68.8, 40.6, 39.8, 39.2, 34.3, 31.4, 29.2, 27.8, 22.6, 22.4, 14.0. HRMS (MALDI, pos. mode, DCTB): calcd for [M-H]$^+$ C$_{141}$H$_{80}$N$_3$O$_{11}$: 1990.579287; found: 1090.57874. Elemental analysis for C$_{141}$H$_{81}$N$_3$O$_{11}$ (1993.17) calcd. C 84.97 H 4.10 N 2.11; found C 82.05, H 4.18, N 2.07.

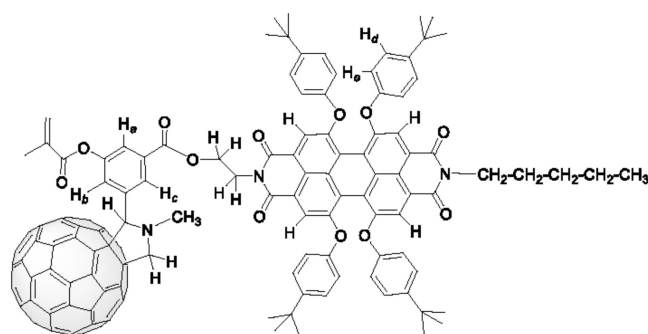**Figure 5.** Formula of dyad **10** for ^{1}H NMR spectrum analysis.

Compound **11**:

To a solution of compound **5** (50 mg, 0.185 mmol) in anhydrous toluene (30 mL) were added C$_{60}$ (220 mg, 0.3 mmol) and sarcosine (60 mg, 0.67 mmol). The reaction mixture was refluxed under nitrogen for 24 h. After the solution was cooled to room temperature, the solvent was removed under reduced pressure and the residue was purified by column chromatography on silica gel. A first column was used to remove the excess C$_{60}$ with CS$_2$, followed by a second one using CH$_2$Cl$_2$. The dyad was isolated as a brown powder (30 mg, 60%). ^{1}H NMR (CDCl$_3$/CS$_2$, 300 MHz, 298 K): 8.00 (br m, 1H), 7.66 (br m, 1H), 7.59 (m, 1H), 7.34 (m, 5H), 5.11 (s, 2H), 5.01 (d, J = 9.3 Hz, 1H), 4.95 (s, 1H), 4.30 (d, J = 9.2 Hz, 1H), 3.90 (s, 3H), 2.80 (s, 3H). MS (MALDI-TOF, pos. mode, dithranol): *m/z*: calcd for: 1017.14; found: 1017.2 [M]$^+$.

Dyad **12**:

To a solution of compound **10** (10 mg, 5.10^{-6} mol) in anhydrous CH_2Cl_2 (2 mL) were added successively freshly distilled Et_3N (7 μL, 5.10^{-5} mol), DMAP (6 mg, 5.10^{-5} mol), then methacryloyl chloride (5 μL, 5.10^{-5} mol). The reaction mixture was stirred at room temperature under argon for 48 h. The residue was purified by silica gel column chromatography using CH_2Cl_2 as the eluent. Dyad **12** was isolated as a purple powder (9.6 mg, 93%).

^{1}H NMR (CDCl$_3$, 300 MHz, 298 K) δ: 8.27 (br s, 2H, H perylene), 8.19 (s, 2H, H perylene), 7.72 (s, 1H, Ha or Hb or Hc), 7.20 and 7.19 (2m, 8H, H$_D$ or H$_E$), 6.80 and 6.75 (2d, ^3J = 8.5 Hz, 8H, H$_D$ or H$_E$), 6.30 (s, 1H, =CH$_2$), 5.71 s, 1H, =CH$_2$), 4.91 (d, J = 9.5 Hz, 1H, -NCH$_2$CH$_2$O-), 4.84 (s, 1H, CH pyrrolidine), 4.75 (br s, 1H, -NCH$_2$CH$_2$O-), 4.63 (br s, 2H, CH$_2$ pyrrolidine), 4.40 (br s, 1H, -NCH$_2$CH$_2$O-), 4.18 (br s, 1H, -NCH$_2$CH$_2$O-), 4.12 (t, J = 7.5 Hz, 2H, NCH$_2$(CH$_2$)$_3$CH$_3$), 2,71 (s, 3H, N-CH$_3$), 2.01 (s, 3H, CH$_3$-C=), 1,67 (m, 2H, -CH$_2$), 1,37 (m, 4H, -CH$_2$CH$_2$-), 1,28 (s, 36H, *t*Bu), 0,90 (t, J = 7 Hz, 3H, CH$_3$) (Figure 6).

Figure 6. Formula of dyad **12** for ^{1}H NMR spectrum analysis.

In agreement with observations for dyad **10**, two protons of the aromatic platform (probably Hb and Hc) were not characterized on the spectrum at 298 K.

^{13}C NMR (CDCl$_3$, 75 MHz, 298 K) δ: 165.5, 163.6, 163.5, 156.3, 155.8, 153.3, 153.0, 152.3, 147.4, 147.2, 146.4, 146.2, 146.1, 146.0, 145.9, 145.7, 145.4, 144.6, 144.4, 142.7, 142.6, 142.2, 142.0, 140.2, 139.5, 139.3, 137.0, 135.8, 135.7, 133.2, 133.1, 127.8, 126.8, 122.7, 122.1, 121.6, 120.8, 120.5, 120.0, 119.6, 119.2, 82.6, 70.0, 69.0, 40.8, 40.0, 34.5, 31.6, 29.8, 29.4, 28.0, 22.6, 18.5, 14.2. HRMS (MALDI, pos. mode, DCTB): calcd for [M-H]$^+$ C$_{145}$H$_{84}$N$_3$O$_{12}$: 2058.604495; found: 2058.6027.

C$_{60}$-PDI Polymer Pol 3:

To a solution of dyad **10** (100 mg) in distilled dioxane (3.5 mL) under argon atmosphere, were added successively Et_3N (10 μL) and poly(methacryloyl chloride) 25% solution in dioxane (Polyscience) (40 μL). The reaction was stirred at room temperature for 24 h before being refluxed for 2 h. The mixture was concentrated under reduced pressure. The product was purified by successive precipitation using CHCl$_3$/CH$_3$OH and CHCl$_3$/hexane.

References

1. Blankenship, R.E.; Tiede, D.M.; Barber, J.; Brudvig, G.W.; Fleming, G.; Ghirardi, M.; Gunner, M.R.; Junge, W.; Kramer, D.M.; Melis, A.; et al. Comparing photosynthetic and photovoltaic efficiencies and recognizing the potential for improvement. *Science* **2011**, *332*, 805–809. [CrossRef] [PubMed]
2. Niklas, J.; Beaupré, S.; Leclerc, M.; Xu, T.; Yu, L.; Sperlich, A.; Dyakonov, V.; Poluektov, O.G. Photoinduced dynamics of charge separation: From photosynthesis to polymer–fullerene bulk heterojunctions. *J. Phys. Chem. B* **2015**, *119*, 7407–7416. [CrossRef] [PubMed]
3. Kroto, H.W.; Heath, J.R.; O'Brien, S.C.; Curl, R.F.; Smalley, R.E. C60: Buckminsterfullerene. *Nature* **1985**, *318*, 162–163. [CrossRef]
4. Krätschmer, W.; Lamb, L.D.; Fostiropoulos, K.; Huffman, D.R. Solid C60: A new form of carbon. *Nature* **1990**, *347*, 354–358. [CrossRef]
5. Kroto, H.W.; Allaf, A.W.; Balm, S.P. C60: Buckminsterfullerene. *Chem. Rev.* **1991**, *91*, 1213–1235. [CrossRef]
6. Langa De La Puente, F.; Nierengarten, J.-F. *Fullerenes: Principles and Applications: Edition 2*; RSC Publishing: Cambridge, UK, 2011.
7. Nierengarten, J.-F. *Fullerenes and Other Carbon-Rich Nanostructures*; Springer: Berlin/Heidelberg, Germany, 2014.
8. Echegoyen, L.; Echegoyen, L.E. Electrochemistry of fullerenes and their derivatives. *Acc. Chem. Res.* **1998**, *31*, 593–601. [CrossRef]
9. Sariciftci, N.S.; Smilowitz, L.; Heeger, A.J.; Wudl, F. Photoinduced electron transfer from a conducting polymer to Buckminsterfullerene. *Science* **1992**, *258*, 1474–1476. [CrossRef]
10. Sariciftci, N.S.; Braun, D.; Zhang, C.; Srdanov, V.I.; Heeger, A.J.; Stucky, G.; Wudl, F. Semiconducting polymer-buckminsterfullerene heterojunctions: Diodes, photodiodes, and photovoltaic cells. *Appl. Phys. Lett.* **1993**, *62*, 585–587. [CrossRef]
11. Hummelen, J.C.; Knight, B.W.; LePeq, F.; Wudl, F.; Yao, J.; Wilkins, C.L. Preparation and characterization of fulleroid and methanofullerene derivatives. *J. Org. Chem.* **1995**, *60*, 532–538. [CrossRef]
12. Dennler, G.; Scharber, M.C.; Brabec, C.J. Polymer-fullerene bulk-heterojunction solar cells. *Adv. Mater.* **2009**, *21*, 1323–1338. [CrossRef]
13. He, Y.; Li, Y. Fullerene derivative acceptors for high performance polymer solar cells. *Phys. Chem. Chem. Phys.* **2011**, *13*, 1970–1983. [CrossRef]
14. Cheng, P.; Zhan, X. Stability of organic solar cells: Challenges and strategies. *Chem. Soc. Rev.* **2016**, *45*, 2544–2582. [CrossRef]
15. Chen, W.; Zhang, Q. Recent progress in non-fullerene small molecule acceptors in organic solar cells (OSCs). *J. Mater. Chem. C* **2017**, *5*, 1275–1302. [CrossRef]
16. Hou, J.; Inganäs, O.; Friend, R.H.; Gao, F. Organic solar cells based on non-fullerene acceptors. *Nat. Mater.* **2018**, *17*, 119–128. [CrossRef]
17. Yan, C.; Barlow, S.; Wang, Z.; Yan, H.; Jen, A.K.Y.; Marder, S.R.; Zhan, X. Non-fullerene acceptors for organic solar cells. *Nat. Rev. Mater.* **2018**, *3*, 18003. [CrossRef]
18. Zhang, G.; Zhao, J.; Chow, P.C.Y.; Jiang, K.; Zhang, J.; Zhu, Z.; Zhang, J.; Huang, F.; Yan, H. Nonfullerene Acceptor Molecules for Bulk Heterojunction Organic Solar Cells. *Chem. Rev.* **2018**, *118*, 3447–3507. [CrossRef]
19. Wadsworth, A.; Moser, M.; Marks, A.; Little, M.S.; Gasparini, N.; Brabec, C.J.; Baran, D.; McCulloch, I. Critical review of the molecular design progress in non-fullerene electron acceptors towards commercially viable organic solar cells. *Chem. Soc. Rev.* **2019**, *48*, 1596–1625. [CrossRef]
20. Zhang, J.; Tan, H.S.; Guo, X.; Facchetti, A.; Yan, H. Material insights and challenges for non-fullerene organic solar cells based on small molecular acceptors. *Nat. Energy* **2018**, *3*, 720–731. [CrossRef]
21. Huber, R. A structural basis of light energy and electron transfer in biology (Nobel Lecture). *Angew. Chem. Int. Ed. Engl.* **1989**, *28*, 848–869. [CrossRef]
22. Wasielewski, M.R. Photoinduced electron transfer in supramolecular systems for artificial photosynthesis. *Chem. Rev.* **1992**, *92*, 435–461. [CrossRef]
23. Gust, D.; Moore, T.; Moore, A. Mimicking photosynthetic solar energy transduction. *Acc. Chem. Res.* **2001**, *34*, 40–48. [CrossRef]
24. Martín, N.; Sánchez, L.; Illescas, B.; Pérez, I. C60-Based electroactive organofullerenes. *Chem. Rev.* **1998**, *98*, 2527–2548. [CrossRef]
25. Huang, C.; Barlow, S.; Marder, S.R. Perylene-3,4,9,10-tetracarboxylic Acid Diimides: Synthesis, Physical Properties, and Use in Organic Electronics. *J. Org. Chem.* **2011**, *76*, 2386–2407. [CrossRef]
26. Nowak-Król, A.; Shoyama, K.; Stolte, M.; Würthner, F. Naphthalene and perylene diimides—better alternatives to fullerenes for organic electronics? *Chem. Commun.* **2018**, *54*, 13763–13772. [CrossRef]

27. Li, C.; Wonneberger, H. Perylene Imides for Organic Photovoltaics: Yesterday, Today, and Tomorrow. *Adv. Mater.* **2012**, *24*, 613–636. [CrossRef]

28. Fernández-Lázaro, F.; Zink-Lorre, N.; Sastre Santos, A. Perylenediimides as non-fullerene acceptors in bulk-heterojunction solar cells (BHJSCs). *J. Mater. Chem. A* **2016**, *4*, 9336–9346. [CrossRef]

29. Shi, Q.; Wu, J.; Wu, X.; Peng, A.; Huang, H. Perylene Diimide-Based Conjugated Polymers for All-Polymer Solar Cells. *Chem. Eur. J.* **2020**, *26*, 12510–12522. [CrossRef]

30. Sharma, V.; Koenig, J.D.B.; Welch, G.C. Perylene diimide based non-fullerene acceptors: Top performers and an emerging class featuring N-annulation. *J. Mater. Chem. A* **2021**, *9*, 6775–6789. [CrossRef]

31. Liu, Z.; Wu, Y.; Zhang, Q.; Gao, X. Non-fullerene small molecule acceptors based on perylene diimides. *J. Mater. Chem. A* **2016**, *4*, 17604–17622. [CrossRef]

32. Rybtchinski, B.; Sinks, L.E.; Wasielewski, M.R. Combining Light-Harvesting and Charge Separation in a Self-Assembled Artificial Photosynthetic System Based on Perylenediimide Chromophores. *J. Amer. Chem. Soc.* **2004**, *126*, 12268–12269. [CrossRef]

33. Nowak-Król, A.; Würthner, F. Progress in the synthesis of perylene bisimide dyes. *Org. Chem. Front.* **2019**, *6*, 1272–1318. [CrossRef]

34. Bingel, C. Cyclopropanierung von fullerenen. *Chem. Ber.* **1993**, *126*, 1957–1959. [CrossRef]

35. Maggini, M.; Scorrano, G.; Prato, M. Addition of azomethine ylides to C60: Synthesis, characterization, and functionalization of fullerene pyrrolidines. *J. Am. Chem. Soc.* **1993**, *115*, 9798–9799. [CrossRef]

36. Nierengarten, J.-F.; Gramlich, V.; Cardullo, F.; Diederich, F. Regio- and diastereoselective bisfunctionalization of C60 and enantioselective synthesis of a C60 derivative with a chiral addition pattern. *Angew. Chem. Int. Ed. Engl.* **1996**, *35*, 2101–2103. [CrossRef]

37. Camps, X.; Hirsch, A. Efficient cyclopropanation of C60 starting from malonates. *J. Chem. Soc. Perkin Trans. 1* **1997**, *11*, 1595–1596. [CrossRef]

38. Hua, J.; Meng, F.; Ding, F.; Li, F.; Tian, H. Novel soluble and thermally-stable fullerene dyad containing perylene. *J. Mater. Chem.* **2004**, *14*, 1849–1853. [CrossRef]

39. Hua, J.; Meng, F.; Ding, F.; Tian, H. Novel soluble and thermally stable perylene dye with two [60]fullerene units. *Chem. Lett.* **2004**, *33*, 432–433. [CrossRef]

40. Wang, N.; Li, Y.; He, X.; Gan, H.; Li, Y.; Huang, C.; Xu, X.; Xiao, J.; Wang, S.; Liu, H.; et al. Synthesis and characterization of a novel electrical and optical-active triads containing fullerene and perylenebisimide units. *Tetrahedron* **2006**, *62*, 1216–1222. [CrossRef]

41. Fortage, J.; Séverac, M.; Houarner-Rassin, C.; Pellegrin, Y.; Blart, E.; Odobel, F. Synthesis of new perylene imide dyes and their photovoltaic performances in nanocrystalline TiO2 dye-sensitized solar cells. *J. Photochem. Photobiol. A* **2008**, *197*, 156–169. [CrossRef]

42. Rybtchinski, B.; Sinks, L.E.; Wasielewski, M.R. Photoinduced Electron Transfer in Self-Assembled Dimers of 3-Fold Symmetric Donor−Acceptor Molecules Based on Perylene-3,4:9,10-bis(dicarboximide). *J. Phys. Chem. A* **2004**, *108*, 7497–7505. [CrossRef]

43. Leroy-Lhez, S.; Baffreau, J.; Perrin, L.; Levillain, E.; Allain, M.; Blesa, M.-J.; Hudhomme, P. Tetrathiafulvalene in a Perylene-3,4:9,10-bis(dicarboximide)-Based Dyad: A New Reversible Fluorescence-Redox Dependent Molecular System. *J. Org. Chem.* **2005**, *70*, 6313–6320. [CrossRef]

44. Leroy-Lhez, S.; Perrin, L.; Baffreau, J.; Hudhomme, P. Perylenediimide derivatives in new donor–acceptor dyads. *C. R. Chim.* **2006**, *9*, 240–246. [CrossRef]

45. Baffreau, J.; Perrin, L.; Leroy-Lhez, S.; Hudhomme, P. Perylene-3,4:9,10-bis(dicarboximide) linked to [60]fullerene as a light-harvesting antenna. *Tet. Lett.* **2005**, *46*, 4599–4603. [CrossRef]

46. Baffreau, J.; Leroy-Lhez, S.; Anh, N.V.; Williams, R.M.; Hudhomme, P. Fullerene C60-perylene-3,4:9,10-bis(dicarboximide) light-harvesting dyads: Spacer-length and bay-substituent effects on intramolecular singlet and triplet energy transfer. *Chem. Eur. J.* **2008**, *14*, 4974–4992. [CrossRef]

47. Baffreau, J.; Leroy-Lhez, S.; Gallego-Planas, N.; Hudhomme, P. Correlation of electrochemical and theoretical parameters in perylenediimide-[60]fullerene dyads. *J. Mol. Struct. THEOCHEM* **2007**, *815*, 145–150. [CrossRef]

48. Hudhomme, P.; Williams, R.M. *Handbook of Carbon Nano Materials*; Electron transfer and applications; D'Souza, F., Kadish, D.M., Eds.; World Scientific Publishing Company: Singapore, 2011; Volume 2.

49. Baffreau, J.; Leroy-Lhez, S.; Hudhomme, P.; Groeneveld, M.M.; van Stokkum, I.H.; Williams, R.M. Superabsorbing fullerenes: Spectral and kinetic characterization of photoinduced interactions in perylenediimide-fullerene-C60 dyads. *J. Phys. Chem. A* **2006**, *110*, 13123–13125. [CrossRef]

50. Baffreau, J.; Leroy-Lhez, S.; Derbal, H.; Inigo, A.R.; Nunzi, J.M.; Groeneveld, M.M.; Williams, R.M.; Hudhomme, P. Light-harvesting fullerenes for organic solar cells. *Eur. Phys. J. Appl. Phys.* **2006**, *36*, 301–305. [CrossRef]

51. Qu, J.; Kohl, C.; Pottek, M.; Müllen, K. Ionic Perylenetetracarboxdiimides: Highly Fluorescent and Water-Soluble Dyes for Biolabeling. *Angew. Chem. Int. Ed.* **2004**, *43*, 1528–1531. [CrossRef]

52. Pla, S.; Martín-Gomis, L.; Ohkubo, K.; Fukuzumi, S.; Fernández-Lázaro, F.; Sastre Santos, A. Macrocyclic dyads based on C60 and perylenediimides connected by click chemistry. *Asian J. Org. Chem.* **2014**, *3*, 185–197. [CrossRef]

53. Martín-Gomis, L.; Peralta-Ruiz, F.; Thomas, M.B.; Fernández-Lázaro, F.; D'Souza, F.; Sastre Santos, A. Multichromophoric perylenediimide-silicon phthalocyanine-C60 system as an artificial photosynthetic analogue. *Chem. Eur. J.* **2017**, *23*, 3863–3874. [CrossRef]

54. Martín-Gomis, L.; Díaz-Puertas, R.; Seetharaman, S.; Karr, P.A.; Fernández-Lázaro, F.; D'Souza, F.; Sastre Santos, Á. Distance Matters: Effect of the Spacer Length on the Photophysical Properties of Multimodular Perylenediimide–Silicon Phthalocyanine– Fullerene Triads. *Chem. Eur. J.* **2020**, *26*, 4822–4832. [CrossRef]

55. Zhu, S.-E.; Liu, K.-Q.; Wang, X.-F.; Xia, A.-D.; Wang, G.-W. Synthesis and properties of axially symmetrical rigid visible light-harvesting systems containing [60]fullerene and perylenebisimide. *J. Org. Chem.* **2016**, *81*, 12223–12231. [CrossRef]

56. Solymosi, I.; Krishna, S.; Nuin, E.; Maid, H.; Scholz, B.; Guldi, D.M.; Pérez-Ojeda, M.E.; Hirsch, A. Diastereoselective formation of homochiral flexible perylene bisimide cyclophanes and their hybrids with fullerenes. *Chem. Sci.* **2021**, *12*, 15491–15502. [CrossRef]

57. Solymosi, I.; Sabin, J.; Maid, H.; Friedrich, L.; Nuin, E.; Perez-Ojeda, M.E.; Hirsch, A. Bis-pseudorotaxane Formation of Perylene Bisimide-Linked [60]Fullerene Dumbbell-Like Molecules with [10]Cycloparaphenylene. *Org. Mater.* **2022**, *4*, 73–85. [CrossRef]

58. Pérez-Ojeda, M.E.; Wabra, I.; Böttcher, C.; Hirsch, A. Fullerene Building Blocks with Tailor-Made Solubility and New Insights into Their Hierarchical Self-Assembly. *Chem. Eur. J.* **2018**, *24*, 14088–14100. [CrossRef]

59. Maxouti, K.L.; Hirsch, A. Sequential Tether-Directed Synthesis of Pentakis-Adducts of C60 with a Mixed [3:2] Octahedral Addition Pattern. *Eur. J. Org. Chem.* **2018**, *2018*, 2579–2586. [CrossRef]

60. Würthner, F. Bay-substituted perylene bisimides: Twisted fluorophores for supramolecular chemistry. *Pure Appl. Chem.* **2006**, *78*, 2341–2349. [CrossRef]

61. Schönamsgruber, J.; Hirsch, A. Benz-Bisimidazole-Bridged Perylenes—Linearly Expanded Chromophores. *Eur. J. Org. Chem.* **2015**, *2015*, 2167–2174. [CrossRef]

62. Kim, W.; Nowak-Król, A.; Hong, Y.; Schlosser, F.; Würthner, F.; Kim, D. Solvent-Modulated Charge-Transfer Resonance Enhancement in the Excimer State of a Bay-Substituted Perylene Bisimide Cyclophane. *J. Phys. Chem. Lett.* **2019**, *10*, 1919–1927. [CrossRef]

63. Shibano, Y.; Umeyama, T.; Matano, Y.; Tkachenko, N.V.; Lemmetyinen, H.; Imahori, H. Synthesis and photophysical properties of electron-rich perylenediimide-fullerene dyad. *Org. Lett.* **2006**, *8*, 4425–4428. [CrossRef]

64. Shibano, Y.; Umeyama, T.; Matano, Y.; Tkachenko, N.V.; Lemmetyinen, H.; Araki, Y.; Ito, O.; Imahori, H. Large reorganization energy of pyrrolidine-substituted perylenediimide in electron transfer. *J. Phys. Chem. C* **2007**, *111*, 6133–6142. [CrossRef]

65. Pla, S.; Martín-Gomis, L.; Fernández-Lázaro, F.; Sastre Santos, A.; Niemi, M.; Lemmetyinen, H.; Tkachenko, N.V. Charge separation and charge recombination photophysical studies in a series of perylene-C60 linear and cyclic dyads. *Phys. Chem. Chem. Phys.* **2016**, *18*, 3598–3605. [CrossRef] [PubMed]

66. Langhals, H. Cyclic carboxylic imide structures as structure elements of high stability. Novel developments in perylene dye chemistry. *Heterocycles* **1995**, *40*, 477–500. [CrossRef]

67. Hofmann, C.C.; Lindner, S.M.; Ruppert, M.; Hirsch, A.; Haque, S.A.; Thelakkat, M.; Köhler, J. Mutual interplay of light harvesting and triplet sensitizing in a perylene bisimide antenna−fullerene dyad. *J. Phys. Chem. B* **2010**, *114*, 9148–9156. [CrossRef] [PubMed]

68. Gómez, R.; Segura, J.L.; Martín, N. Highly efficient light-harvesting organofullerenes. *Org. Lett.* **2005**, *7*, 717–720. [CrossRef] [PubMed]

69. Bamford, W.R.; Stevens, T.S. The decomposition of toluene-p-sulphonylhydrazones by alkali. *J. Chem. Soc.* **1952**, *28*, 4735–4740. [CrossRef]

70. Wienk, M.M.; Kroon, J.M.; Verhees, W.J.H.; Knol, J.; Hummelen, J.C.; van Hal, P.A.; Janssen, R.A.J. Efficient methano[70]fullerene/ MDMO-PPV bulk heterojunction photovoltaic cells. *Angew. Chem. Int. Ed.* **2003**, *42*, 3371–3375. [CrossRef]

71. Xiao, S.; Li, Y.; Li, Y.; Zhuang, J.; Wang, N.; Liu, H.; Ning, B.; Liu, Y.; Lu, F.; Fan, L.; et al. [60]Fullerene-based molecular triads with expanded absorptions in the visible region: Synthesis and photovoltaic properties. *J. Phys. Chem. B* **2004**, *108*, 16677–16685. [CrossRef]

72. Li, Y.; Wang, N.; He, X.; Wang, S.; Liu, H.; Li, Y.; Li, X.; Zhuang, J.; Zhu, D. Synthesis and characterization of ferrocene-perylenetetracarboxylic diimide–fullerene triad. *Tetrahedron* **2005**, *61*, 1563–1569. [CrossRef]

73. Wu, Y.; Li, Y.; Li, H.; Shi, Q.; Fu, H.; Yao, J. N-type cascade electron transfer along an oxidative gradient. *Chem. Commun.* **2009**, *45*, 6955–6957. [CrossRef]

74. Li, Y.; Li, Y.; Liu, H.; Wang, S.; Wang, N.; Zhuang, J.; Li, X.; He, X.; Zhu, D. Self-assembled monolayers of porphyrin–perylenetetracarboxylic diimide–[60] fullerene on indium tin oxide electrodes: Enhancement of light harvesting in the visible light region. *Nanotechnology* **2005**, *16*, 1899–1904. [CrossRef]

75. Würthner, F.; Stepanenko, V.; Chen, Z.; Saha-Möller, C.R.; Kocher, N.; Stalke, D. Preparation and characterization of regioisomerically pure 1,7-disubstituted perylene bisimide dyes. *J. Org. Chem.* **2004**, *69*, 7933–7939. [CrossRef]

76. Liu, Y.; Wang, N.; Li, Y.; Liu, H.; Li, Y.; Xiao, J.; Xu, X.; Huang, C.; Cui, S.; Zhu, D. A new class of conjugated polyacetylenes having perylene bisimide units and pendant fullerene or porphyrin groups. *Macromolecules* **2005**, *38*, 4880–4887. [CrossRef]

77. Lu, F.; Xiao, S.; Li, Y.; Liu, H.; Li, H.; Zhuang, J.; Liu, Y.; Wang, N.; He, X.; Li, X.; et al. Synthesis and chemical properties of conjugated polyacetylenes having pendant fullerene and/or porphyrin units. *Macromolecules* **2004**, *37*, 7444–7450. [CrossRef]

78. Dubey, R.K.; Niemi, M.; Kaunisto, K.; Efimov, A.; Tkachenko, N.V.; Lemmetyinen, H. Direct evidence of significantly different chemical behavior and excited-state dynamics of 1,7- and 1,6-regioisomers of pyrrolidinyl-substituted perylene diimide. *Chem. Eur. J.* **2013**, *19*, 6791–6806. [CrossRef]

79. Kaunisto, K.M.; Vivo, P.; Dubey, R.K.; Chukharev, V.I.; Efimov, A.; Tkachenko, N.V.; Lemmetyinen, H.J. Charge-transfer dynamics in poly(3-hexylthiophene):perylenediimide-C60 blend films studied by ultrafast transient absorption. *J. Phys. Chem. C* **2014**, *118*, 10625–10630. [CrossRef]

80. Hahn, U.; Nierengarten, J.-F.; Delavaux-Nicot, B.; Monti, F.; Chiorboli, C.; Armaroli, N. Fullerodendrimers with a perylenediimide core. *New J. Chem.* **2011**, *35*, 2234–2244. [CrossRef]

81. Serin, J.M.; Brousmiche, D.W.; Fréchet, J.M.J. A FRET-based ultraviolet to near-infrared frequency converter. *J. Amer. Chem. Soc.* **2002**, *124*, 11848–11849. [CrossRef]

82. Felder, D.; Nierengarten, H.; Gisselbrecht, J.-P.; Boudon, C.; Leize, E.; Nicoud, J.-F.; Gross, M.; Van Dorsselaer, A.; Nierengarten, J.-F. Fullerodendrons: Synthesis, electrochemistry and reduction in the electrospray source for mass spectrometry analysis. *New J. Chem.* **2000**, *24*, 687–695. [CrossRef]

83. Hahn, U.; Hosomizu, K.; Imahori, H.; Nierengarten, J.-F. Synthesis of dendritic branches with peripheral fullerene subunits. *Eur. J. Org. Chem.* **2006**, *2006*, 85–91. [CrossRef]

84. Chamberlain, T.W.; Davies, E.S.; Khlobystov, A.N.; Champness, N.R. Multi-electron-acceptor dyad and triad systems based on perylene bisimides and fullerenes. *Chem. Eur. J.* **2011**, *17*, 3759–3767. [CrossRef] [PubMed]

85. Liu, Y.; Zhao, J. Visible light-harvesting perylenebisimide–fullerene (C60) dyads with bidirectional "ping-pong" energy transfer as triplet photosensitizers for photooxidation of 1,5-dihydroxynaphthalene. *Chem. Commun.* **2012**, *48*, 3751–3753. [CrossRef] [PubMed]

86. Rocard, L.; Hudhomme, P. Recent Developments in the Suzuki–Miyaura Reaction Using Nitroarenes as Electrophilic Coupling Reagents. *Catalysts* **2019**, *9*, 213. [CrossRef]

87. Rocard, L.; Hatych, D.; Chartier, T.; Cauchy, T.; Hudhomme, P. Original Suzuki–Miyaura Coupling Using Nitro Derivatives for the Synthesis of Perylenediimide-Based Multimers. *Eur. J. Org. Chem.* **2019**, *2019*, 7635–7643. [CrossRef]

88. Rocard, L.; Goujon, A.; Hudhomme, P. Nitro-Perylenediimide: An Emerging Building Block for the Synthesis of Functional Organic Materials. *Molecules* **2020**, *25*, 1402. [CrossRef] [PubMed]

89. Hruzd, M.; Rocard, L.; Goujon, A.; Allain, M.; Cauchy, T.; Hudhomme, P. Desymmetrization of Perylenediimide Bay Regions Using Selective Suzuki–Miyaura Reactions from Dinitro Substituted Derivatives. *Chem. Eur. J.* **2020**, *26*, 15881–15891. [CrossRef] [PubMed]

90. El-Berjawi, R.; Hudhomme, P. Synthesis of a perylenediimide-fullerene C60 dyad: A simple use of a nitro leaving group for a Suzuki-Miyaura coupling reaction. *Dye. Pigm.* **2018**, *159*, 551–556. [CrossRef]

91. Uno, M.; Ban, H.S.; Nabeyama, W.; Nakamura, H. de novo Design and synthesis of N-benzylanilines as new candidates for VEGFR tyrosinekinase inhibitors. *Org. Biomol. Chem.* **2008**, *6*, 979–981. [CrossRef]

92. Coco, S.; Cordovilla, C.; Donnio, B.; Espinet, P.; García-Casas, M.J.; Guillon, D. Self-organization of dendritic supermolecules, based on isocyanide–gold(I), –copper(I), –palladium(II), and –platinum(II) complexes, into micellar cubic mesophases. *Chem. Eur. J.* **2008**, *14*, 3544–3552. [CrossRef]

93. Zhao, H.; Thurkauf, A. A practical and convenient synthesis of methyl 5-formyl-3-methoxybenzoate. *Synth. Commun.* **2001**, *31*, 1921–1926. [CrossRef]

94. Neises, B.; Steglich, W. Simple Method for the Esterification of Carboxylic Acids. *Angew. Chem. Int. Ed. Engl.* **1978**, *17*, 522–524. [CrossRef]

95. Diacon, A.; Derue, L.; Lecourtier, C.; Dautel, O.; Wantz, G.; Hudhomme, P. Cross-linkable azido C60-fullerene derivatives for efficient thermal stabilization of polymer bulk-heterojunction solar cells. *J. Mater. Chem. C* **2014**, *2*, 7163–7167. [CrossRef]

96. Boovanahalli, S.K.; Kim, D.W.; Chi, D.Y. Application of ionic liquid halide nucleophilicity for the cleavage of ethers: A green protocol for the regeneration of phenols from ethers. *J. Org. Chem.* **2004**, *69*, 3340–3344. [CrossRef]

97. Bieliauskas, A.V.; Weerasinghe, S.V.W.; Pflum, M.K.H. Structural requirements of HDAC inhibitors: SAHA analogs functionalized adjacent to the hydroxamic acid. *Bioorg. Med. Chem. Lett.* **2007**, *17*, 2216–2219. [CrossRef]

98. Haberkorn, N.; Kim, S.; Kim, K.-S.; Sommer, M.; Thelakkat, M.; Sohn, B.-H.; Theato, P. Template-Assisted Fabrication of Highly Ordered Interpenetrating Polymeric Donor/Acceptor Nanostructures for Photovoltaic Applications. *Macromol. Chem. Phys.* **2011**, *212*, 2142–2150. [CrossRef]

99. Lindner, S.M.; Thelakkat, M. Nanostructures of n-Type Organic Semiconductor in a p-Type Matrix via Self-Assembly of Block Copolymers. *Macromolecules* **2004**, *37*, 8832–8835. [CrossRef]

100. Sommer, M.; Thelakkat, M. Synthesis, characterization and application of donor-acceptor block copolymers in nanostructured bulk heterojunction solar cells. *Eur. Phys. J. Appl. Phys.* **2006**, *36*, 245–249. [CrossRef]

101. Sommer, M.; Lindner, S.M.; Thelakkat, M. Microphase-Separated Donor–Acceptor Diblock Copolymers: Influence of HOMO Energy Levels and Morphology on Polymer Solar Cells. *Adv. Funct. Mater.* **2007**, *17*, 1493–1500. [CrossRef]

102. Sommer, M.; Lang, A.S.; Thelakkat, M. Crystalline-crystalline donor-acceptor block copolymers. *Angew. Chem. Int. Ed. Engl.* **2008**, *47*, 7901–7904. [CrossRef]

103. Hüttner, S.; Sommer, M.; Thelakkat, M. n-type organic field effect transistors from perylene bisimide block copolymers and homopolymers. *Appl. Phys. Lett.* **2008**, *92*, 093302. [CrossRef]

104. Huettner, S.; Sommer, M.; Hodgkiss, J.; Kohn, P.; Thurn-Albrecht, T.; Friend, R.H.; Steiner, U.; Thelakkat, M. Tunable Charge Transport Using Supramolecular Self-Assembly of Nanostructured Crystalline Block Copolymers. *ACS Nano* **2011**, *5*, 3506–3515. [CrossRef] [PubMed]

105. Yuen, J.D.; Pozdin, V.A.; Young, A.T.; Turner, B.L.; Giles, I.D.; Naciri, J.; Trammell, S.A.; Charles, P.T.; Stenger, D.A.; Daniele, M.A. Perylene-diimide-based n-type semiconductors with enhanced air and temperature stable photoconductor and transistor properties. *Dye. Pigm.* **2020**, *174*, 108014. [CrossRef]

106. Aoki, H.; Takahashi, T.; Tamai, Y.; Sekine, R.; Aoki, S.; Tani, K.; Ito, S. Poly(methacrylate)s labeled by perylene diimide: Synthesis and applications in single chain detection studies. *Polym. J.* **2009**, *41*, 778–783. [CrossRef]

107. Davis, N.J.L.K.; MacQueen, R.W.; Roberts, D.A.; Danos, A.; Dehn, S.; Perrier, S.; Schmidt, T.W. Energy transfer in pendant perylene diimide copolymers. *J. Mater. Chem. C* **2016**, *4*, 8270–8275. [CrossRef]

108. Sato, H.; Matsuda, D.; Ogino, K. Synthesis and polymerization of methacrylate having fullerene. *Polym. J.* **1998**, *30*, 904–909. [CrossRef]

109. Zheng, J.; Goh, S.H.; Lee, S.Y. Synthesis and thermal properties of fullerene-containing polymethacrylates. *Polym. Bull.* **1997**, *39*, 79–84. [CrossRef]

110. Kurmaz, S.V.; Ozhiganov, V.V. Fullerene-containing branched polymethacrylates and polymer networks: Synthesis, structure, and properties. *Polym. Sci. Ser. A* **2011**, *53*, 232–245. [CrossRef]

111. Lopatin, M.A.; Evlampieva, N.P.; Lopatina, T.I.; Kuznetsova, Y.L.; Lavrenko, P.N. Methyl methacrylate polymerization in the presence of C60 (C70) and molecular characteristics of fullerene-containing poly(methyl methacrylate). *Russ. J. Gen. Chem.* **2008**, *78*, 1545–1552. [CrossRef]

112. Lin, Q.; Xu Xu, R.H.J.; Yang, N.; Karim, A.A.; Loh, X.J.; Zhang, K. UV Protection and Antioxidant Activity of Nanodiamonds and Fullerenes for Sunscreen Formulations. *ACS Appl. Nano Mater.* **2019**, *2*, 7604–7616. [CrossRef]

113. Heuts, J.P.A.; Gilbert, R.G.; Maxwell, I.A. Penultimate Unit Effect in Free-Radical Copolymerization. *Macromolecules* **1997**, *30*, 726–736. [CrossRef]

114. Günther, H.; Guenther, H. *NMR Spectroscopy: An Introduction*; Wiley Publishing: New York, NY, USA, 1980.

115. Du, H.; Fuh, R.-C.A.; Li, J.; Corkan, L.A.; Lindsey, J.S. *Photochemistry and Photobiology*; Wiley Publishing: New York, NY, USA, 1998; Volume 68, pp. 141–142.